Physics – Uspekhi **53** (5) 455 – 479 (2010)

INSTRUMENTS AND METHODS OF INVESTIGATION PACS numbers: 41.20.Jb, 42.25.Bs, 42.30.Wb, 43.20.Gp

Invisible cloaking of material bodies using the wave flow method

A E Dubinov, L A Mytareva

DOI: 10.3367/UFNe.0180.201005b.0475

Contents

Abstract. The current knowledge of the physics of electromagnetic cloaking of material objects by the wave flow method is reviewed. Experiments demonstrating the feasibility of this cloaking method are described. Some aspects of calculating cloak profiles are examined, and achievements and unsolved problems in the theory of the interaction of electromagnetic waves with shells are considered. Prospects for developing the cloaking method for waves of other physical nature (acoustic and probability density waves) are discussed.

A E Dubinov, L A Mytareva Sarov State Institute of Physics and Technology, ul. Dukhova 6, 607186 Sarov, Nizhny Novgorod region, Russian Federation
Tel. (7-83130) 45 144, (7-83130) 51 235
E-mail: dubinov-ae@yandex.ru, mytareva-la@yandex.ru

Received 19 August 2009, revised 3 December 2009
Uspekhi Fizicheskikh Nauk **180** (5) 475 – 501 (2010)
DOI: 10.3367/UFNr.0180.201005b.0475
Translated by E G Strel'chenko; edited by A Radzig

1. Introduction

How to become invisible or make things less visible has always been a subject of extreme interest to people. The dream of becoming fully invisible is found in the fairytales of many countries and is featured in fantasy novels and movies. Every possible invisibility cloaks and caps of darkness, as well as similar fairytale 'devices' made fictional heroes invisible and gave them many advantages.

The dream of invisibility and attempts at bringing it to life have continued into our times. Indeed, 20th century advances in radar and sonar technology intensified these attempts. The practical significance of this activity is well exemplified by stealth technology, in which the object to be concealed is given either a special shape or a special solid shell.

In the last two or three years, major breakthroughs that have been made in this area, both conceptual and methodological, have raised the promise that invisibility technology is a matter of the very near future. It is accepted that the masking method to be discussed was invented by Sir Pendry, an Imperial College London expert in electrodynamics of left-handed media and metamaterials [1, 2], and that his invention

is based on the mathematical work of Ulf Leonhardt, also of the UK [3, 4]. Terminologically, the approach can be called the '*wave flow method*', as aptly suggested by the Russian physicist N N Rozanov [5]; the term *cloaking* was assigned to Pendry's method in English language literature.

The breakthrough in cloaking triggered what can safely be called a boom among specialists. Theoretical papers applying the wave flow method to ever new cloaking schemes have been and are being published at an explosive rate (several per week currently), and as of now ten plus laboratories are engaged in a bitter race for leadership in the field.

By now, cloaking research using the wave flow method has advanced enough to allow summaries to be made, key achievements to be analyzed, and challenges to be identified. However, there are as yet no reviews or books exclusively devoted to wave flow method, and in some reviews [6, 7] only a brief mention is made of it. A popular paper [5] and a brief undergraduate-level text [8] on the subject should perhaps also be mentioned here.

This paper aims to present all information available as of late 2009 on achievements and problems in the field of wave masking.

Some important remarks are in order before proceeding to the main body of the paper. The way things are, many of those who gave heard or read about the new cloaking method strongly associate it with the concepts of a left-handed medium and negative refraction (as many newspaper reports and popular science papers do). The point is, in our view, that Pendry and his coworkers proposed using elements of metamaterials (magnetic composite media) as their cloaking coatings. Metamaterials were first created in the late 1990s and have since been intensively investigated precisely as media which exhibit negative refraction at certain frequencies (left-handed media). However, as far as their operating frequency range is concerned, cloaking metamaterials mostly behave as normal, right-handed materials.

The wave flow method itself, as we shall see below, does not necessarily rely on negative refraction materials — at least not for simple cloak geometries like the sphere, cylinder, etc. For this reason, the physics of left-handed media and metamaterials will not be considered here, and the interested reader is referred to review papers [9–14], monographs [15–17], and popular science books [18, 19].

As a final remark: it is known that new is often well-forgotten old. In concluding the paper we shall argue (see Appendix III) that the wave flow concept had been around long before metamaterials came along, so that attempts to implement it with conventional right-handed media may have been undertaken as far back as the middle of the last century.

2. Masking methods

There are a variety of methods that have been developed for masking material objects, for concealing and making them less visible. In presenting these methods in this section we shall in part follow the review by Rozanov [5], presenting additional illustrative examples if need be.

In the optical range, the principal method to avoid observation is, of course, *camouflage* (or the *color matching* of the background), which hampers detecting or recognizing objects optically, by the eye or some device. While camouflage coloration does not make an object invisible and only reduces its contrast with the background, it forces the observer to spend some time to detect the object, even when knowing its approximate location beforehand. Camouflage clothing used by hunters and the military is a common example of this color matching. In the animal world, there are many ways of blending into the background, including the following: *cryptic coloration* to match the environment (e.g., green lizards, grasshoppers, and caterpillars in grass, brownish-yellow locusts or saigas on sand, polar bears and snow leopards against snow, age and seasonal moulting in hares and fur-seals); *disruptive coloration*, when contrasting coloration helps concealment in a complex-relief environment (zebras, chipmunks); *concealing coloration* based on the light-shadow effect in which the more illuminated parts (say, top) of an animal's body are relatively darker in color, as is the case with many animals.

One further way nature suggests as a means to achieve invisibility is by matching environment in terms of properties other than color. For example, in jellyfish and 'normal' fish the body index of refraction is nearly equal to that of sea water. Objects with this property are practically invisible, even under very close observation. This idea was used by Mr Griffin, the hero of H Wells's *The Invisible Man*, who self-injected some chemicals to make the index of refraction of his body equal to that of the ambient air. Unfortunately, this property cannot be imparted to any desired object, and this approach has very limited applicability.

The advent of radar greatly extended the concept of invisibility. Before that, 'invisible' meant hidden from visual sight; today, it can also stand for hidden from radar.

What primarily distinguishes radar from optical cloaking is that in order to see an object a radar locator emits its own radiation and if the object completely absorbs this radiation — and hence no reflected wave comes back — the radiation seems to have disappeared into nothing. In other words, the object is invisible. The eye, unlike radar, uses light from an external source to see an object, so that an object coated with an absorbent is black in color and is therefore very visible against almost any background.

Another cloaking technique is to utilize scattering coatings. For example, stealth technology gives aircraft a specific angular shape to cause the incident radio radiation to be scattered in a direction totally different from backward direction to the source (this shape, incidentally, markedly deteriorates the aerodynamic performance of the aircraft). In the optical range, in contrast, a scattering coating does not make an object invisible but only blurs its outline.

However, cloaking technologies like stealth are less efficient if there is more than one radar, so that the radiation emitted by one of them enters the field of sight of another when reflected from the object. A system of locators allows even absorbing objects to be detected: each of the radars sees things illuminated not only by its own light but also by light from an external source, so that an object that absorbs radiation will be visible — in the same way that black object is visible to the eye against a white background.

Detection technology, for its part, has been keeping pace with cloaking technologies in recent decades: whatever new cloaking method is developed, a new method of detecting objects by indirect evidence (such as shadow, scattering radiation, or aircraft wake) quickly emerged. There is, therefore, an acute need for cloaking procedure which would minimize this evidence.

In recent years, a number of new cloaking schemes have been proposed. Of these, owing to its universal nature,

particular development has gone into the wave flow method, which is the subject of the next section.

3. The idea of the wave flow method

In 2006, J Pendry and colleagues came up with a fundamentally new invisibility concept [1, 2]. Their basic idea was that a cloaking shell should curve the wave front of the incident electromagnetic radiation so as to cause it to bend around the object and to assume its original direction on the opposite side of the object (Fig. 1). Externally, then, it looks as if there is nothing on the path of the wave, i.e., what the observer sees is not a cloaked object but rather empty space behind it.

For the observer to notice no indications of nonuniformity, it is also necessary that the optical path of each ray in the shell be the same as if the ray had propagated along a straight line in free space. Otherwise, the rays that have passed through the cloak simply will not fall into the general picture: they will interfere with those that have not interacted with the cloak and thus will distort the field pattern.

The proposed way to implement the idea is by making use of cloaking material nonuniformities. Indeed, it is a well-known phenomenon that a ray of light undergoes refraction at the interface between two media. But if the refractive index varies continuously in the medium, the refraction of the ray is continuous and the ray trajectory is a smooth curve. This, incidentally, is the explanation of the well-known phenomenon of mirage, in which objects beyond the horizon are seen. This kind of a mirage is observed in calm, dry, and very hot weather, when in the layer of stagnant air near the ground there is a clearly defined radial distribution (or gradient) of refractive index. As a result, the rays of light curve around the surface of the Earth, allowing one to see things beyond the horizon and leaving invisible the Earth's surface between the observer and the mirage.

The question now arises: How can those values of the cloak material parameters (specifically, the permittivity and permeability tensors) which will yield the desired ray trajectories be calculated? Reference [1] suggests a procedure which is no less fascinating than light bending itself: to mentally create a curved-metric space within a shell, for which purpose it is necessary to find the transformation of coordinates. Underlying the procedure is the fact that Maxwell's equations remain invariant under spatial transformations (see Appendix I).

This procedure is most easily explained by the following simple example. Suppose we need an invisibility cloak shaped like a spherical layer $R_1 < r < R_2$, the surrounding medium being vacuum (or air). Let us make the transformation which maps a sphere of radius R_2 with its center at the origin of

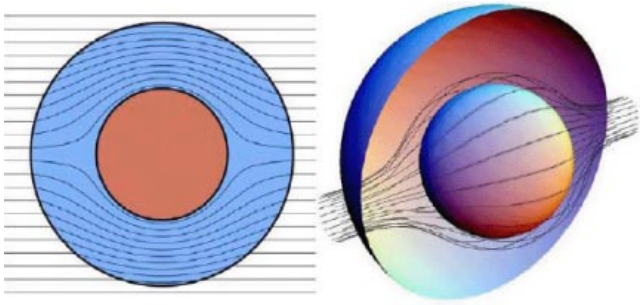

Figure 1. Ray trajectories in the cloak [1].

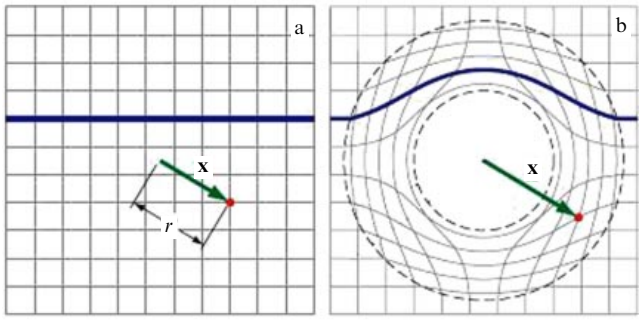

Figure 2. Straight line and vector **x** in the original (Cartesian) coordinate system. (b) Cartesian grid, the same line and vector in new coordinates (taken from Ref. [20]).

coordinates onto this layer:

$$r' = R_1 + r\,\frac{R_2 - R_1}{R_2}\,, \qquad \theta' = \theta\,, \qquad \varphi' = \varphi\,. \tag{1}$$

Under this transformation, Maxwell's equations

$$\nabla \times \mathbf{E} = -\frac{1}{c}\,\frac{\partial \mathbf{H}}{\partial t}\,, \qquad \nabla \times \mathbf{H} = \frac{1}{c}\,\frac{\partial \mathbf{E}}{\partial t} \tag{2}$$

formally retain their appearance:

$$\nabla \times \tilde{\mathbf{E}} = -\frac{\hat{\mu}}{c}\,\frac{\partial \tilde{\mathbf{H}}}{\partial t}\,, \qquad \nabla \times \tilde{\mathbf{H}} = \frac{\hat{\varepsilon}}{c}\,\frac{\partial \tilde{\mathbf{E}}}{\partial t}\,, \tag{3}$$

where $\tilde{\mathbf{E}}$ and $\tilde{\mathbf{H}}$ are the fields in the new coordinates, and $\hat{\mu}$ and $\hat{\varepsilon}$ are tensors with diagonal components

$$\varepsilon_{rr} = \mu_{rr} = \frac{R_2}{R_2 - R_1}\,\frac{(r - R_1)^2}{r^2}\,, \qquad \varepsilon_{\theta\theta} = \mu_{\theta\theta} = \frac{R_2}{R_2 - R_1}\,,$$
$$\varepsilon_{\phi\phi} = \mu_{\phi\phi} = \frac{R_2}{R_2 - R_1} \tag{4}$$

(the general expressions for an arbitrary transformation are derived in Appendix I).

Because the equations have identical forms, so too will their solutions with respect to their coordinate systems. This means that a medium that was given a parameter distribution (4) will bend a straight ray just as the transformation (1) bends a straight line intersecting a sphere of radius $r < R_2$ (Fig. 2).

Because, further, the transformation did not affect the time region, it follows that at any instant of time the phases of every ray will be the same in the original and transformed systems. Thus, using this coordinate transformation, we obtained the parameters of a cloak which satisfies all the invisibility requirements we have listed above.

It should be noted that an equivalent effect could be produced by so-called antigravitation were it existent in nature. Antigravitation in the presence of a repelling body deforms the metric of space in such a way that geodesics, in a sense, move apart (as opposed to moving closer together in conventional gravitation).

From Eqns (4), which are a purely mathematical result, it is seen that the components of the permittivity and permeability, $\varepsilon_{rr} = \mu_{rr}$, assume values less than unity (which could in fact be said without deriving Eqns (4) because the geometric path a ray travels in the cloaking shell is longer than in a vacuum, whereas the optical paths and phase incursions should be equal).

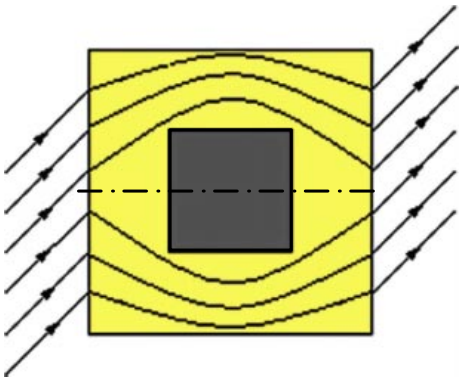

Figure 3. Schematic illustrating the incidence of rays on a rectangular cross section cloaking shell (shown in white); incidence is from left to right.

Calculations for shapes other than spherical (for example, for a cube) predict negative values for some permittivity and permeability components. This is illustrated graphically in Fig. 3, where the rays traveling above the dash-and-dot line (which divides the rectangle in half) refract when entering the cloak: as usual, the incident and refracted rays are on opposite sides of the normal to the interface. The rays traveling below the dash-and-dot line refract negatively: the incident ray and the refracted ray appear on the same side of the normal, i.e., here we already need a left-handed medium. At the same time, it is readily understood that, when incident on a cloaking shell with a circular cross section, any ray will refract positively.

Negative refraction is also necessarily present in cloaks of many other shapes. This is especially true of nonconvex (for example, heart-shaped) shells, which we shall consider below. On the other hand, it is clear that, if need be, any body (even a nonconvex one) can be cloaked by a spherical shell of sufficiently large radius, meaning that there is no need for left-handed media!

However, and this can be seen from Eqn (4), what is really needed for cloaking by the wave flow method is anisotropic gradient materials with permittivity and permeability components less than unity or (in some cases) negative. In what follows we shall examine how the ideas in this section can be put into practice.

Note. Thus, a cloaking shell is an anisotropic medium. The question that arises here is why each of the rays refracts in its own unique way. And, noting that anisotropic media generally lift the polarization degeneration of a wave, which rays are usual and which are unusual?

According to the authors of the method, this preservation of polarization degeneracy is due to the fact that the permittivity and permeability tensors of the cloak material are equal [20]. If, it is argued, the cloaking medium is a transformed vacuum with the same properties ($\varepsilon = \mu = 1$) and if, further, there is only one way in which a vacuum refracts a ray, how can the cloak possibly split the ray in two?

Added to the above general arguments, the authors of Ref. [20] prove quite rigorously that a cloaking shell cannot be birefrigent. Defining the operator $\hat{K}$ by the expression

$$\mathbf{k} \times \left(\hat{\mu}^{-1}(\mathbf{k} \times \mathbf{E})\right) + \hat{\varepsilon}\mathbf{E} = \hat{K}\mathbf{E} \tag{5}$$

and denoting $\hat{\varepsilon} = \hat{\mu} = \hat{n}$, they obtain a dispersion relation for the cloak in the form

$$\det\left(\hat{K}\hat{n}^{-1}\hat{K} + \hat{n}\right) = \frac{1}{\det \hat{n}}\left(\mathbf{k}\hat{n}\mathbf{k} - \det \hat{n}\right)^2 . \tag{6}$$

Although equation (6) is of the fourth order in **k**, it has only two (opposite-sign) solutions. In birefrigent media, in contrast, all four solutions of the dispersion equation are different.

4. First experimental demonstration of wave flow cloaking

The first implementation of wave flow cloaking using a metamaterial coating deserves a separate story. It is in large part the success of these experiments which generated a wave of interest in this method in the scientific community, and it is these experiments which identified the key cloaking problems which have been the focus of attention of experts for the last two or three years.

Preceding these experiments was the numerical simulation in Ref. [21] of flow around an infinitely long cylindrical shell with a circular cross section. The interaction of the shell with a linearly polarized electromagnetic wave was simulated with the finite-differences time-domain (FDTD) method, which does not use the geometrical-optics approximation and yields the wave-field pattern in its entirety (full-wave simulation).

The parameters of the cylindrical cloak were calculated by the method of coordinate transformation

$$\varepsilon_{rr} = \mu_{rr} = \frac{r-a}{r}, \qquad \varepsilon_{\phi\phi} = \mu_{\phi\phi} = \frac{r}{r-a}, \qquad \varepsilon_{zz} = \mu_{zz} = \left(\frac{b}{b-a}\right)^2 \frac{r-a}{r}, \tag{7}$$

using the linear transformation

$$r' = \frac{b-a}{b}\, r + a, \qquad \varphi' = \varphi, \qquad z' = z, \tag{8}$$

where a and b are the inner and outer radii of the cylindrical shell, respectively.

The interaction of a linearly polarized wave with this cloak is illustrated in Fig. 4a for the wave vector **E** parallel to the cylinder axis. The cloaking effect does show up here: the radiation does not penetrate the cavity and is virtually

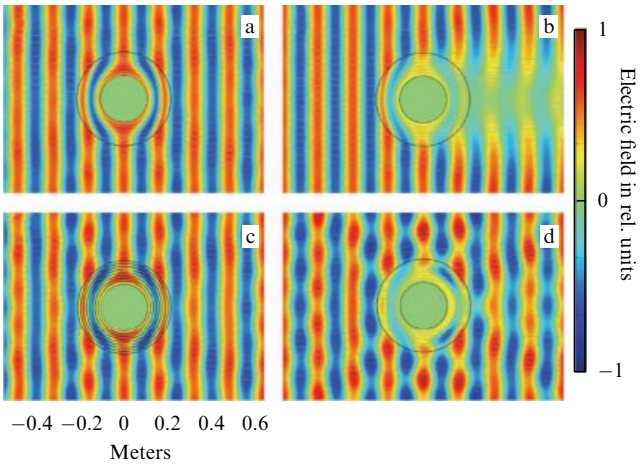

Figure 4. Normalized amplitude distribution for an electric field near a cylindrical cloak. Thin vertical lines indicate ray trajectories; power flow in all cases is from left to right. (a) Coating with ideal parameters (7), (b) the same with a loss tangent of 0.1, (c) eight-layer approximation of the perfect coating, and (d) coating with simplified parameters (12). (Taken from Ref. 21].) (For a colored version see http://www.ufn.ru.)

unscattered by the cloaking surface, and the wave front becomes plane again after the wave has passed the shell.

Because the calculations in Ref. [21] were a lead-up to experiments, the perfect cloaking shell remained out of consideration. Recognizing that a cloaking shell with continuously variable parameters and no dissipative losses is beyond practical possibility, the authors also modelled the interaction of a plane wave with a layered coating (eight layers, each with its own refractive index) and with a lossy coating.

From Fig. 4b it is seen that a discrete shell somewhat deteriorates the picture (rays of light are no longer straight lines outside the shell due to scattering) and that nonzero absorption gives rise to a shadow.

Unfortunately, a cloak with the parameters shown in Eqn (7) is thus far very difficult to obtain because all the permittivity and permeability components are spatially nonuniform. However, if, for example, the incident vector **E** is parallel to the cylinder axis z, the problem becomes two-dimensional and the z-components of the permittivity and permeability tensors can be assumed constant ($D_z = \varepsilon_{zz} E_z$, $\varepsilon_{zz} = \text{const}$). Then, Maxwell's equations inside the shell become

$$\mathrm{i}\omega D_z = \frac{1}{r}\left[\frac{\partial(rH_\varphi)}{\partial r} - \frac{\partial H_r}{\partial \varphi}\right], \tag{9}$$

$$\mathrm{i}\omega \mu_{rr} H_r = \frac{1}{r}\frac{\partial(D_z/\varepsilon_{zz})}{\partial \phi}, \tag{10}$$

$$\mathrm{i}\omega \mu_{\phi\phi} H_\phi = -\frac{\partial(D_z/\varepsilon_{zz})}{\partial r}. \tag{11}$$

The permittivity and permeability components enter Eqns (9)–(11) through the products $\mu_{rr}\varepsilon_{zz}$ and $\mu_{\phi\phi}\varepsilon_{zz}$, so that, instead of the parameters given by Eqn (7), one can apply simpler expressions which give the same result.

Reference [21] suggests the following set of parameters:

$$\varepsilon_{zz} = \left(\frac{b}{b-a}\right)^2, \quad \mu_{rr} = \left(\frac{r-a}{r}\right)^2, \quad \mu_{\phi\phi} = 1. \tag{12}$$

This, of course, makes things much simpler because here only one component is spatially nonuniform! Referring to Fig. 4d, which shows a cloak with parameters (12), the curved ray trajectories outside the shell indicate that scattering in all directions is rather strong. Nevertheless, the cloaking effect shows itself here, because radiation still does not penetrate the region of $r < a$.

The cloak prepared for the experiments of Ref. [2] (published shortly after Ref. [21] by the same team of researchers) possessed all the nonidealities listed above, i.e., simplified material parameters (12), discreteness, and absorption. In addition, the cylinder had a finite (and very small) height.

The coating comprised ten layers, each consisting of a very large number of ring resonators, which is the most widespread metamaterial structural element. The geometrical size of the resonators was specific for each layer and chosen so as to make the $\mu_{rr}(r)$ the closest possible to the parameters (12). The radii of the layers were chosen such that the circumference of a layer contains an integer number of resonators. The shell and the parameters of its elements are shown in Figs 5 and 6. A hollow conducting

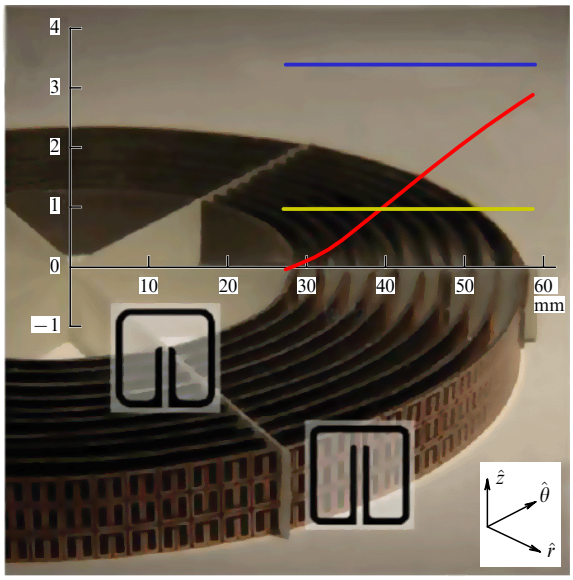

Figure 5. Cylindrical cloaking shell (background image) with plots of $\mu_{rr}(r)$ (slanted line), $\mu_{\phi\phi}(r)$ (lower horizontal straight line), and $\varepsilon_{zz}(r)$ (upper horizontal line). (Taken from Ref. [2].)

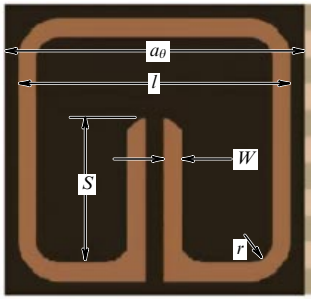

N	r	s	μ_{rr}
1	0.260	1.654	0.003
2	0.254	1.677	0.023
3	0.245	1.718	0.052
4	0.230	1.771	0.085
5	0.208	1.825	0.120
6	0.190	1.886	0.154
7	0.173	1.951	0.188
8	0.148	2.027	0.220
9	0.129	2.110	0.250
10	0.116	2.199	0.279

Figure 6. Geometric parameters of ring resonators (N is the layer number). (Taken from Ref. [2].)

cylinder of radius $r = 0.26$ m was taken as an object to be cloaked.

The experimental results presented in Fig. 7 demonstrate that, despite all its shortcomings, a cylindrical shell still has some cloaking effect, i.e., reduces the visibility of the cloaked object: a conducting cylinder covered with this shell scatters radiation much less than when not covered (cf. Figs 7a and 7b). It was this first success that became the starting point for a new approach to cloaking technology.

5. Other possibilities for choosing parameters for a circular cross section cylindrical cloak

Reference [21] employed linear transformation (8) to obtain permittivity and permeability components (7). There are, however, an infinitely large number of ways to transform a solid cylinder to a hollow one; the linear transformation was chosen entirely because of its simplicity.

The transformation for a cylindrical shell has the following general form:

$$r' = f(r), \quad \varphi' = \varphi, \quad z' = z, \quad f(a) = 0, \quad f(b) = b. \tag{13}$$

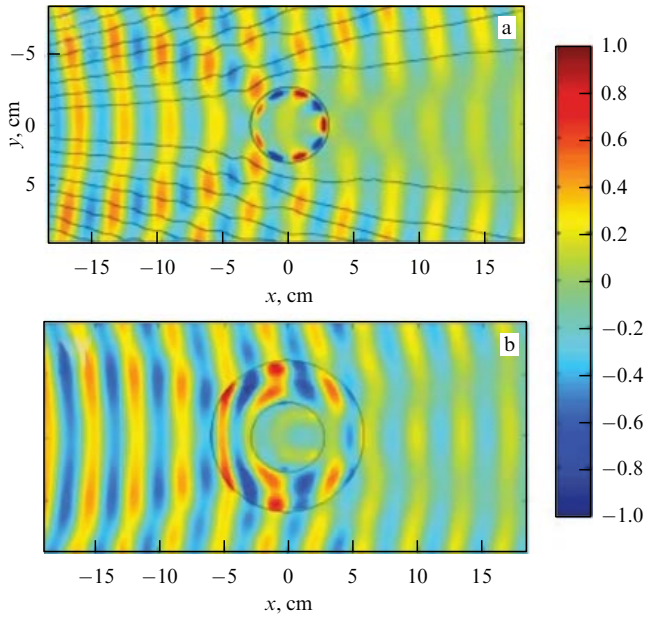

Figure 7. Normalized amplitude distribution for an electric field: (a) experimental measurement for a bare cylinder (thin black lines indicate the direction of power flow), and (b) experimental measurement for a cloaked cylinder. (Taken from Ref. [2].)

The permittivity and permeability components then are calculated as

$$\varepsilon_{rr} = \mu_{rr} = \frac{f(r)}{rf'(r)}\,, \qquad \varepsilon_{\phi\phi} = \mu_{\phi\phi} = \frac{rf'(r)}{f(r)}\,, \qquad \varepsilon_{zz} = \mu_{zz} = \frac{f(r)\,f'(r)}{r}\,, \tag{14}$$

where $f'(r) = \mathrm{d}f(r)/\mathrm{d}r$ (relations (14) follow from the general expressions for the $\hat{\varepsilon}$ and $\hat{\mu}$ tensors derived in Appendix I).

A perfect cloaking effect can be achieved with a linear transformation, provided only that the cloak is fabricated with parameters (7). In practice, however, this has turned out to be extremely challenging, so a great deal of attention has been given to how to decrease the number of nonuniform components in the $\hat{\varepsilon}$ and $\hat{\mu}$ tensors.

The first attempt — the one that led to parameters (12) — proved unsatisfactory because the shell caused too large a scattering (Fig. 4d). A better result was obtained in Refs [22, 23], where, strange as it may seem, more complex transformations were applied to create simpler cloaks.

Reference [22], dealing with the quadratic transformation

$$r' = f(r) = \frac{-ar^2 + (b^2 + a^2)r - ab^2}{(b-a)^2}\,, \tag{15}$$

offers the following set of cloaking shell parameters:

$$\varepsilon_{rr} = \frac{(b^2 - ra)^2 (r-a)^2}{(b-a)^4 r^2}\,, \qquad \varepsilon_{\phi\phi} = \frac{(a^2 + b^2 - 2ra)^2}{(b-a)^4}\,, \qquad \mu_{zz} = 1\,. \tag{16}$$

These expressions were obtained by analogy with Eqn (12) but for a different polarization of incident radiation (vector **B** is parallel to the z-axis).

There are two important advantages to this set of parameters over Eqn (12). First, the outer surface impedance of the shell matches that of the surrounding medium, viz.

$$Z\big|_{r=b} = \sqrt{\frac{\mu_{zz}}{\varepsilon_{\phi\phi}}}\,\bigg|_{r=b} = 1\,, \tag{17}$$

resulting in a cloak with the parameters given in Eqn (16) scattering incident radiation much less than a simplified cloak with parameters (12). Second, because $\mu_z = 1$, the cloak can be considered nonmagnetic for a wave with this polarization (see above; the absence of magnetic properties in the medium usually greatly simplifies the practical solution to the problem). Therefore, despite the complex expressions for the $\hat{\varepsilon}$ components, parameters (16) seem, by and large, to be simpler to implement than parameters (7).

The authors of Ref. [23] attacked the problem from a somewhat different angle, by putting the transformation, on the contrary, as the function $r = g(r')$,

$$r = g(r') = \left[\frac{a}{b}\left(\frac{r'}{b} - 2\right) + 1\right] r' + a\,, \tag{18}$$

and arriving ultimately at the following set of simplified parameters for the case of the incident radiation with the vector **B** parallel to the z-axis:

$$\varepsilon_{rr} = \left(\frac{r'}{r}\right)^2, \qquad \varepsilon_{\phi\phi} = \left[\frac{\partial g(r')}{\partial r'}\right]^{-2}, \qquad \mu_{zz} = 1\,. \tag{19}$$

A shell with parameters (19), while advantageously nonmagnetic and impedance-matched with its surroundings, is disadvantageous in having a limitation on the thickness: $a/b < 0.5$ (otherwise transformation (13) would be nonmonotonic).

Reference [23] also carried out efficiency comparisons between the linear nonmagnetic cloak with transformation $g(r') = (1 - a/b)r' + a)$, the quadratic nonmagnetic cloak with $g(r')$ given by Eqn (18), and the perfect linear cloak with parameters (7) (see Fig. 8). It can be concluded that higher-order transformations give a very good result: the quadratic nonmagnetic cloak scatters much less radiation than the linear nonmagnetic cloak.

6. Cloak shape diversity

Experiments with a cylindrical shell launched an avalanche of calculations for other cloak geometries. It should be noted that all the published results have been numerical simulations: real cloaks of sufficient quality have been beyond the technology of the time. With the exception of the first, proof-of-principle experiment, imperfect technologies have made the experiments meaningless because the resulting picture would be too blurred to draw conclusions concerning geometry-related properties of the cloaks.

Let us have a look at what has been done in this area.

Note, to start with, that any object placed within a cylindrical shell will be hidden by it just as effectively as by a spherical one. True, for most practical applications a cylinder is inconvenient and, for example, a spherical cloak is more universal, but because noncylindrical cloaks are complicated to simulate they, for a long time, have been given much less attention.

For a wave incident normally on the cylindrical shell (the wave front is parallel to the cylinder generatrix) there is no

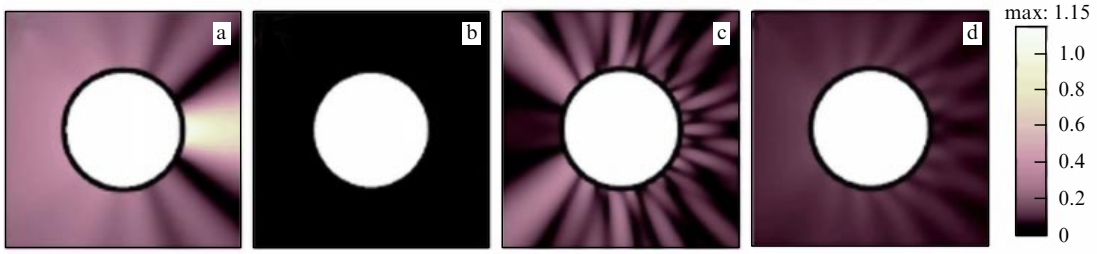

Figure 8. Normalized amplitude distribution for radiation scattered from (a) a bare conducting cylinder, (b) a perfect cloak, (c) a linear nonmagnetic shell, and (d) a quadratic nonmagnetic cloak. (Taken from Ref. [23])

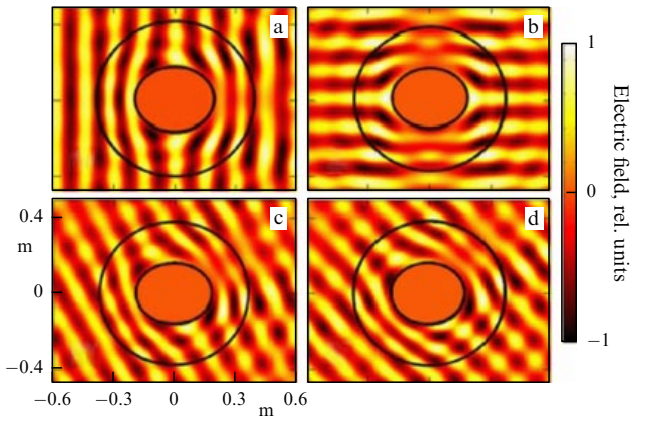

Figure 9. Normalized amplitude distribution for the electric field of radiation incident on an elliptic shell for various angles of incidence: (a) 0°, (b) 90°, (c) 30°, (d) 45° (taken from Ref. [24]).

field energy flow along the generatrix, so that the field pattern is the same for any cross section, i.e., is planar (the reason they are called 2D-cylindrical). It should be noted, however, that this problem cannot strictly be considered two-dimensional because the cylindrical shell has clearly defined permittivity and permeability components ε_{zz} and μ_{zz}, where the z-axis is parallel to the cylinder's generatrix [see expressions (7)]. Still, such plane (in a sense) problems are much less cumbersome than fully three-dimensional ones. In fact, it is due to this relative simplicity that cylindrical cloaks have been given such attention.

In what follows, the key shell geometries that have been investigated are reviewed.

6.1 Elliptic cylinder

One of the simplest elliptic-cylindrical cloaks was considered in Ref. [24] (Fig. 9). The parameters of this cloak are calculated using a linear transformation of the elliptic-cylindrical coordinates $x = c\xi\eta$, $y = c[(\xi^2 - 1)(1 - \eta^2)]^{1/2}$, $z = z$, which squeezes a solid elliptical cylinder into a cylinder with a cavity:

$$\xi' = \xi_1 + (\xi - 1)\,\frac{\xi_2 - \xi_1}{\xi_2 - 1}\,, \qquad \eta' = \eta\,, \qquad z' = z\,. \tag{20}$$

As noted in Ref. [24], because the elliptic cylinder exhibits smaller degree of symmetry than the circular one, it is not indifferent to the incident radiation direction. From Fig. 9, which shows situations for different angles of incidence relative to the major axis of the ellipse, it is apparent that the maximum cloaking effect is achieved at a zero angle of incidence.

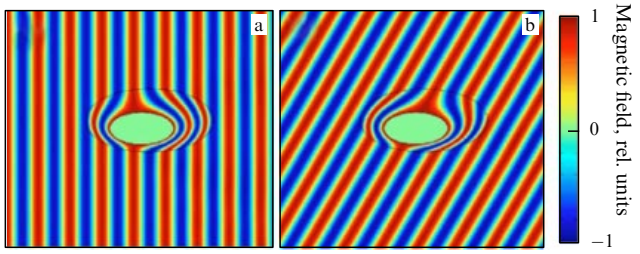

Figure 10. Normalized amplitude distribution for the magnetic field of radiation incident on an eccentric elliptic shell for various angles of incidence: (a) 0°, and (b) 30° (taken from Ref. [25]).

A more general, asymmetric elliptical shell was treated in Ref. [25] (Fig. 10). Curiously, despite the complete absence of symmetry, such a shell produces the cloaking effect for any direction of radiation incidence.

The cloaking effect can be achieved by properly choosing the coordinate system and the transformation. For this purpose, the authors of Ref. [25] introduced their own non-orthogonal (!) system of coordinates (q_1, q_2, q_3) related to (x, y, z) by the relationships

$$q_1 = \sqrt{\left(\frac{x - q_1 x_c}{a}\right)^2 + \left(\frac{y - q_1 y_c}{b}\right)^2}\,, \qquad q_2 = \arctan\frac{(y - q_1 y_c)/b}{(x - q_1 x_c)/a}\,, \quad q_3 = z\,. \tag{21}$$

Here, the coordinate lines $q_1 = \text{const}$ (in the xy plane) are ellipses with equal semiminor-to-semimajor axis ratio b/a, both centered at $(x, y) = (q_1 x_c, q_1 y_c)$, and the coordinate lines $q_2 = \text{const}$ are radial lines passing through point $(0, 0)$ (Fig. 11a). The linear transformation

$$(q_1', q_2', q_3') = \left(1 + \frac{s - 1}{s}\,q_1, q_2, q_3\right), \quad 0 \leqslant q_1 \leqslant s\,, \tag{22}$$

maps an elliptic cylinder to one with an eccentric cavity (see Fig. 11b). Because the coordinate system (q_1, q_2, q_3) is not orthogonal, it follows that the $\hat{\varepsilon}$ and $\hat{\mu}$ tensors of this cloak calculated by coordinate transformation method have off-diagonal components $\varepsilon_{12} = \varepsilon_{21} = \mu_{12} = \mu_{21}$ (the expressions in Ref. [25] are too unwieldy to be reproduced here).

Reference [25] demonstrated convincingly that nonsymmetric shells can by all means produce a symmetric cloaking effect, provided only a necessary (admittedly very complex) parameter distribution was created in them.

In Ref. [26], the same authors presented another curious generalization of the elliptical cloaking concept, a uniform-thickness elliptic-cylindrical layer (Fig. 12). An interesting

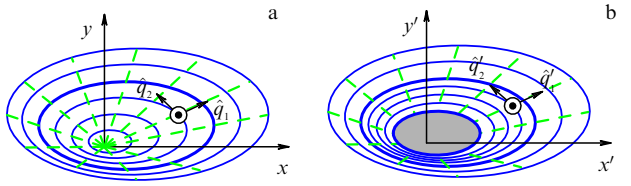

Figure 11. Coordinate systems for an eccentric elliptic shell: (a) coordinate system (q_1, q_2, q_3) with coordinate lines $q_1 = \text{const}$ (solid) and $q_2 = \text{const}$ (dashed), and (b) coordinate system (q_1', q_2', q_3') with corresponding coordinate lines (taken from Ref. [25]).

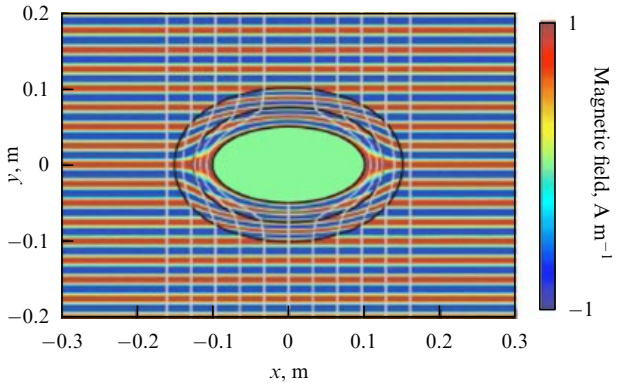

Figure 12. Normalized amplitude distribution for a magnetic field of radiation incident on a uniform-thickness elliptic cloak (taken from Ref. [26]).

point about this geometry is that the inner and outer surfaces of the cloaking layer are not similar figures, which adds complications of its own and also necessitates the transformation of nonorthogonal coordinates.

The convenience of the elliptic geometry is its universality: depending on the semiaxis ratio, the ellipse changes from very elongated to nearly perfectly circular and can therefore be used in a wide variety of practical applications. This point is brought to attention in Ref. [27], which derives $\hat{\varepsilon}$ and $\hat{\mu}$ tensors for a concentric elliptic shell.

The following expressions are reproduced from Ref. [27] for reference purposes:

$$\varepsilon_{xx} = \frac{r_1}{r_1 - ka} + \frac{k^2a^2R^2 - 2kar_1^3}{(r_1 - ka)r_1^5}\, x^2\,, \tag{23a}$$

$$\varepsilon_{xy} = \frac{k^2a^2R^2 - 2ka(1+k^2)r_1^3}{(r_1 - ka)r_1^5}\, xy = \varepsilon_{yx}\,, \tag{23b}$$

$$\varepsilon_{yy} = \frac{r_1}{r_1 - ka} + \frac{k^2a^2R^2 - 2k^3ar_1^3}{(r_1 - ka)r_1^5}\, y^2\,, \tag{23c}$$

$$\varepsilon_{zz} = \left(\frac{b}{b-a}\right)^2 \frac{r_1 - ka}{r_1}\,. \tag{23d}$$

Here, k is the major-to-minor semiaxis ratio, the same for the inner and outer ellipses; a and b are their minor semiaxes; $r_1 = (x^2 + k^2y^2)^{1/2}$; and $R = (x^2 + k^4y^2)^{1/2}$.

Although the shape of the shell is the same as in Ref. [24], Ref. [27] uses a more complex, nonlinear transformation:

$$(x', y') = \left[\frac{b-a}{b} + \frac{ka}{\sqrt{x^2 + k^2y^2}}\right] x, y\,, \quad z' = z\,.$$

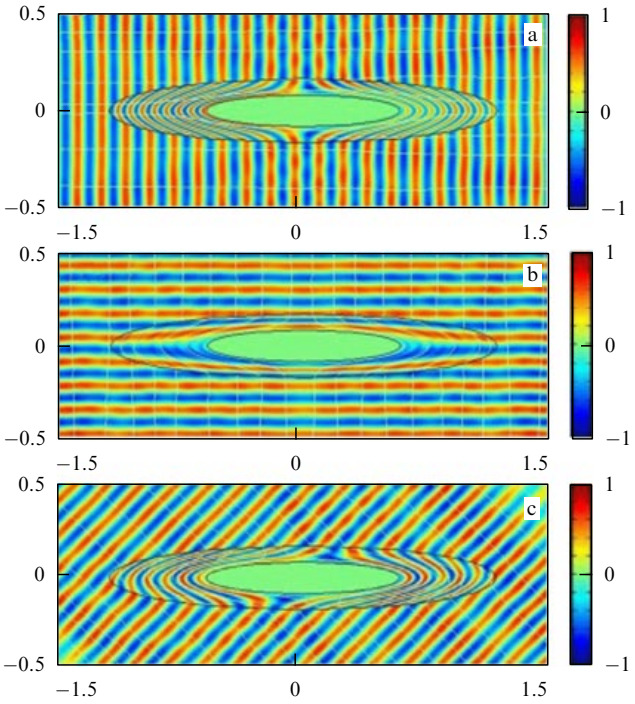

Figure 13. Normalized amplitude distribution for an electric field of radiation incident on an elliptic shell for various angles of incidence relative to the horizontal axis: (a) 0°, (b) 90°, and (c) 45° (taken from Ref. [27]).

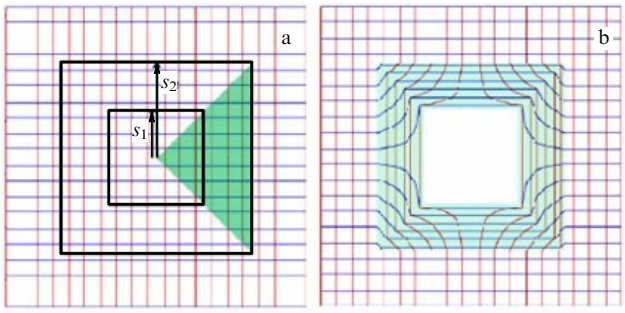

Figure 14. Coordinate transformation for a square cross section cylindrical shell; each sector marked in panel 'a' is subject to its own coordinate transformation (taken from Ref. [28]).

As a result, such a shell produces a symmetric cloaking effect (Fig. 13).

6.2 Arbitrary cylinder

The method of coordinate transformations can also be applied to calculate the parameters for any shape of a shell. However, in this general case there is no transformation that will map a simply connected region onto its similar doubly connected one (for example, if the boundary of the region is a broken line). Then, tensors $\hat{\varepsilon}$ and $\hat{\mu}$ are defined piecewise by making a number of transformations simultaneously.

For a simple example, we can consider a cylindrical shell of square cross section, whose parameters were calculated in Ref. [28]. Here, transformations are made and material parameters assigned for each 'sector' of the square specifically (Fig. 14).

A more complex broken-line boundary can also be cut into pieces, and for each of these its own transformation can be made, similar to what was done in Ref. [29] (Fig. 15).

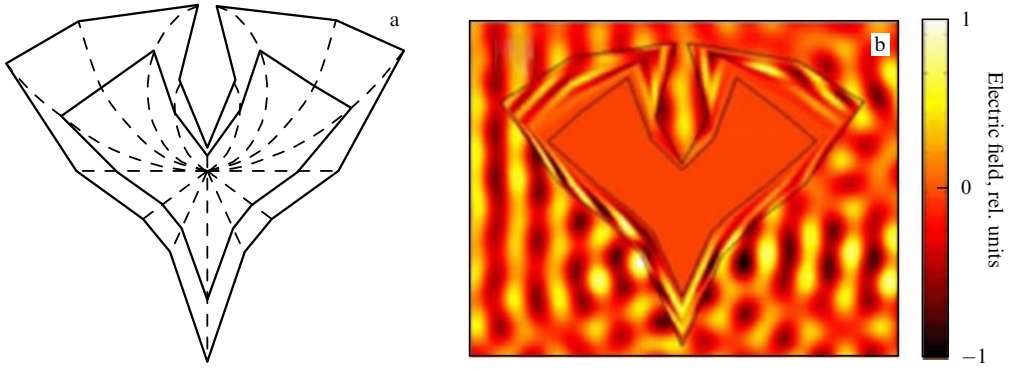

Figure 15. Bird-shaped broken-line-boundary cloaking shell: (a) outline, (b) normalized amplitude distribution for the electric field of radiation incident horizontally on such a shell (taken from Ref. [29]).

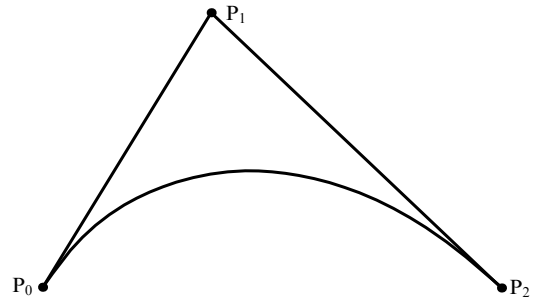

Figure 16. Second-order Bezier curve with three control points: P_0, P_1, and P_2 (taken from Ref. [30]).

Fortunately, with current computational technologies a large number of such operations can be carried out in a short period of time. This method can also be applied to calculating two-dimensional shells with smoothly curved boundaries (in which case a curvilinear boundary should be approximated by a broken line).

The nonuniform rational B-spline (NURBS) method used in Ref. [30] is more accurate in this sense. In this method, the smooth boundary of the cloaking shell is approximated by a combination of several second-order Bezier curves (which, depending on the parameters, may represent any conical cross sections, including ellipses, parabolas, or hyperbolas).

A second-order Bezier curve is defined by specifying three points, $P_0(a_0, b_0)$, $P_1(a_1, b_1)$, and $P_2(a_2, b_2)$ (Fig. 16) and three parameters, w_0, w_1, and w_2, which are called weights. The parametric equations of the curve have the form

$$x(u) = \frac{w_0 a_0 (1-u)^2 + 2w_1 a_1 (1-u)u + w_2 a_2 u^2}{w_0 (1-u)^2 + 2w_1 (1-u)u + w_2 u^2}\,, \qquad (24a)$$

$$y(u) = \frac{w_0 b_0 (1-u)^2 + 2w_1 b_1 (1-u)u + w_2 b_2 u^2}{w_0 (1-u)^2 + 2w_1 (1-u)u + w_2 u^2}\,. \qquad (24b)$$

This method, although seemingly more complex than the broken-line method, has the weighty advantage that, for a smooth curve to be approximated to sufficient accuracy, one needs a broken curve consisting of hundreds of segments, whereas for Bezier curves this number is much fewer. For example, the heart shape needs only two Bezier curves for its description: one for the left half, and one for the right half (Fig. 17). Curiously, these curves were developed quite recently, in the 1960s, by Pierre Bezier, a French engineer at Renault working on approximating aerodynamic car shapes.

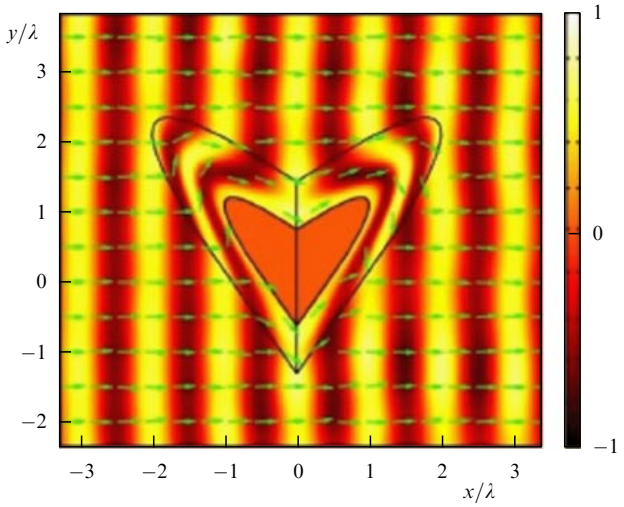

Figure 17. Normalized amplitude distribution for the electric field of radiation incident on a heart-shaped cloaking shell; arrows indicate the direction of the power flow (taken from Ref. [30]).

Reference [31] suggests yet another interesting method for calculating cylindrical shells with an arbitrary cross section. The equations of the outer and inner shell boundaries (in the plane of the transverse cross section) are specified in polar coordinates

$$f_{\text{in}}(\varphi) = a\rho(\varphi)\,, \qquad (25)$$

$$f_{\text{out}}(\varphi) = b\eta(\varphi)\,, \qquad (26)$$

where $\rho(\varphi)$ and $\eta(\varphi)$ are dimensionless functions, and a and b are the 'radii' or scale coefficients (figures specified by equations with the same function $\rho(\varphi)$ but different 'radii' are similar). Then, a transformation linear in r of a singly connected region with boundary f_{out} into a doubly connected region with boundaries f_{out} and f_{in} takes the form

$$r' = a + \frac{b\eta(\varphi) - a\rho(\varphi)}{b\eta(\varphi)}\, r\,. \qquad (27)$$

The approach suggested in Ref. [31] is interesting in allowing the inner and outer shell surfaces to be nonsimilar. Figure 18 demonstrates, as an example, the cloaking effect of one of the shells with parameters obtained by this method.

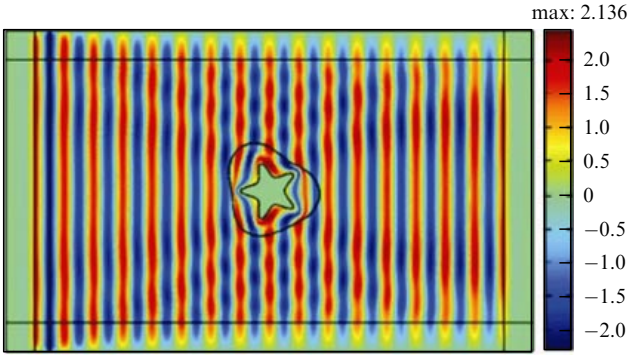

Figure 18. Normalized amplitude distribution of the electric field for a cylindrical cloaking shell with both the outer and inner boundaries arbitrarily shaped (taken from Ref. [31]).

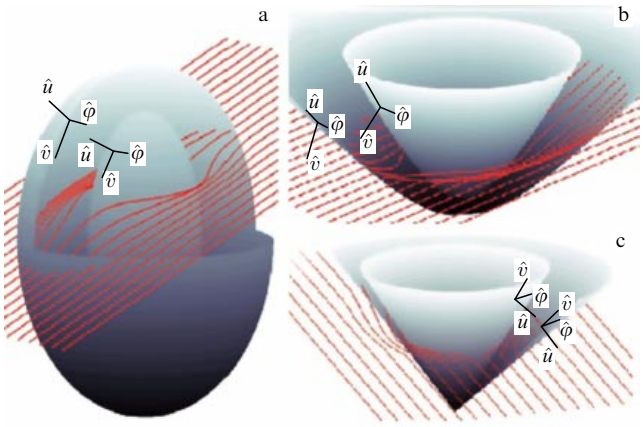

Figure 19. Passage of rays through cloaking shells in the form of (a) a spheroid, (b) a hyperboloid (taken from Ref. [32]), and (c) a cone (taken from Ref. [33]).

The essential features of this cloak are that, first, the object being cloaked is not convex, and, second, details of its geometry are less than a wavelength in size.

6.3 Three-dimensional shells

Only a limited number of three-dimensional shell studies have been conducted, none of them for an arbitrary shape. The reason, as mentioned above, is that such problems are difficult to model. Besides the very first spherical shape suggested, ellipsoids of rotation (Fig. 19a), open hyperboloids (Fig. 19b), and open cones (Fig. 19c) were investigated [32, 33].

7. Key challenges of wave flow cloaking

Some obstacles on the way to creating 'invisibility cloaks' by using coordinate transformations were pointed out as early as Ref. [1], and the experimental studies of Refs [2] and [21] confirmed that they are indeed serious. Let us list them here.

7.1 Dispersion

We have already mentioned that, the optical paths being equal, the geometric path of a ray in a cloaking shell is longer than in a vacuum. This means, in fact, that the phase velocity of a wave in the cloak is larger than the speed of light in a vacuum, c. Because the group velocity cannot exceed c, this means that it does not equal the phase velocity, which in itself implies the presence of frequency dispersion [$\varepsilon_{ij} = \varepsilon_{ij}(\omega)$, $\mu_{ij} = \mu_{ij}(\omega)$]. Thus, the cloaking shell can only be fully efficient at a single frequency — one for which the permittivity and permeability components take the appropriate forms [for example, Eqn (4) for a spherical shell]. Moreover, the cloaking material itself can be dispersive to a greater or lesser degree, depending on its structure.

All this could be avoided by performing cloaking not in a vacuum but in a medium of higher optical density (with a refractive index of $n = 5$, for example). Cloaking requires materials with a refractive index less than that of the surrounding medium, i.e., in this case usual materials with $1 < n < 5$ will do. Unfortunately, this is hardly applicable in practice, where one is normally concerned with cloaking in the air, but even now some demonstration experiments are possible.

7.2 Dissipative losses

As can be seen from Fig. 4b, an absorbing cloak (as indeed any other radiation-absorbing object) casts a shadow and so gives the cloaked object up. Losses in the cloaking shell are unavoidable primarily due to the rather strong dispersion in it. The well-known Kramers–Kronig relations imply that the imaginary part of the permittivity (permeability) is higher as the rate at which its real part varies with frequency increases. That is, media with high dispersion in a certain frequency range have high absorption in this range.

7.3 Situations with permittivity and permeability components becoming zero or infinite

Let us take another look at expressions (4). We note that $\varepsilon_{rr} = \mu_{rr} = 0$ at the inner surface of the spherical cloak. The same is true for the cylindrical shell. Thus, the whole of the inner surface consists of singular points, which greatly compounds any electromagnetic problem.

One way to deal with singular points is by choosing an appropriate coordinate transformation. For example, Ref. [34], which offers yet another version of an elliptical cylinder cloak, uses a linear transformation of the classical coordinates of an elliptic cylinder, for which confocal ellipses serve as coordinates lines in the plane of the transverse cross section (Fig. 20). Recall that other cylindrical shell studies make other choices for coordinate ellipses (for example, in Ref. [27] the semiaxis ratio is taken to be a constant).

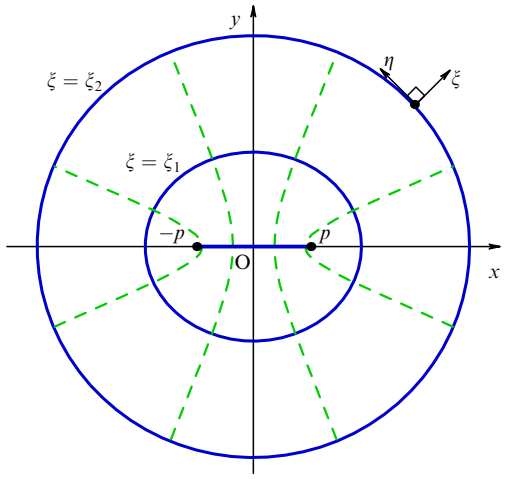

Figure 20. Coordinate system for an elliptic cylinder (taken from Ref. [34]).

In Ref. [34], it is argued that whether singular points exist or not depends on what the measure is of that set of points which the coordinate transformation 'inflates' into a cavity. There are no singular points if the original set of points and its image have the same measure. Because the image is always a surface (the inner surface of the shell), it follows that the original set should also have measure 2.

This requirement is not satisfied for the spherical cloaking shell obtained by transformation (1) because its cavity 'grows' from the center of the sphere (set of measure zero). For a circular cylindrical shell [transformation (8)], the inner surface is obtained from the cylinder's axis (the straight line is a set of measure 1). The same is the case for the elliptic cylindrical shells discussed in Section 6. As a result, all these cloaking shells have singular points at their inner surfaces.

In contrast to them, the inner surface of the elliptic shell proposed in Ref. [34] is obtained from a region in a plane (the segment $[-p, p]$ in the cross section shown in Fig. 20), so that the permittivity and permeability components never become zero in this region.

8. Overcoming dispersion and anisotropy: plane layer cloaking

Thus, we have seen that frequency dispersion is an inalienable property of a cloaking shell, which at the same time prevents the shell from being perfect. It is then logically expected that the smoother the frequency dependences of the permittivity and permeability components $\varepsilon_{ij}(\omega)$, $\mu_{ij}(\omega)$, the lower the absorption and hence the better the cloaking effect. In this context, an important issue is finding an optimal coordinate transformation that minimizes the dispersion, while preserving the cloaking properties of the shell.

The search for such a transformation is the subject of Ref. [35], where the degree of dispersion of a cloak is considered to be directly dependent on the degree of its anisotropy. The authors reformulated the problem into one of smoothing out the anisotropy by appropriately shaping the cloak and choosing a coordinate transformation.

The title of Ref. [35], "Hiding under the Carpet: A New Strategy for Cloaking", graphically presents the authors' idea: cloaking against the background of a smooth surface using a plane layer which has an indentation on its lower surface where the object to be hidden is placed (Fig. 21).

The following is the procedure for finding a transformation which maps a rectangle $w \times h$ into a rectangle with an indentation and which produces the minimum anisotropy in doing so. The first step in this procedure is assuming that the cloaking layer reflects radiation in the same way as a dielectric plate with $\varepsilon = \varepsilon_{\text{ref}}$ and $\mu = 1$.

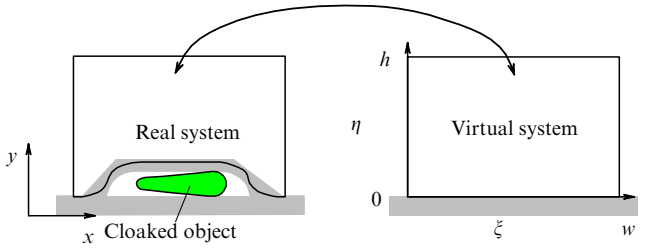

Figure 21. Real and virtual systems, the term virtual meaning how things appear to the observer (taken from Ref. [35]).

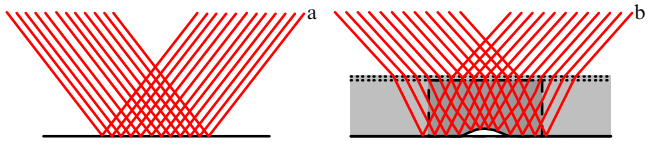

Figure 22. Trajectories of rays incident (a) on the background surface, and (b) on the cloaking layer (taken from Ref. [36]).

This being so, the cloak itself is visible in a medium with $\varepsilon = 1$ and $\mu = 1$ (unlike the cloaks in all the preceding cases) and is transparent, but the observer cannot even imagine there is an object under the layer and all they see is the 'floor' (similar to circus tricks with mirrors).

The cloaking shell may indeed be made totally invisible by coating its top and ends with a so-called impedance-matching layer, in which the refractive index varies linearly from $n_0 = 1$ at the outer surface to $n = \sqrt{\varepsilon_{\text{ref}}}$ at the inner surface. The impedances at the interfaces then turn out to be matched, so there is no reflection from them and all the parts of the system, except for the background surface, become invisible (Fig. 22).

At the next step, the authors of Ref. [35] consider an arbitrary transformation, corresponding to the conditions of the problem, from the Cartesian coordinates (x, y) to curvilinear coordinates (ξ, η) and arrive at the following expressions for the permittivity and permeability:

$$\varepsilon = \frac{\varepsilon_{\text{ref}}}{\sqrt{\det g}}, \qquad [\mu^{ij}] = \frac{\Lambda\Lambda^{\text{T}}}{\sqrt{\det g}}. \tag{28}$$

Here, Λ is the transformation matrix, and $g = \Lambda^{\text{T}}\Lambda$ is the transformation metric (we note that ε is a scalar quantity which is a function of the coordinates, and that $[\mu^{ij}]$ is a tensor whose components are also spatially inhomogeneous).

Next, the so-called '*anisotropy factor*'

$$\alpha = \max\left(\frac{n_{\text{T}}}{n_{\text{L}}}, \frac{n_{\text{L}}}{n_{\text{T}}}\right) \tag{29}$$

is introduced, where $n_{\text{T,L}} = \sqrt{\varepsilon\mu_{\text{T,L}}}$ are the refractive indices along the principal axes of the permeability tensor, and μ_{T} and μ_{L} are its principal values.

The larger the value of α, the stronger the anisotropy. Accordingly, the problem reduces to finding such a coordinate transformation for which the anisotropy factor α (dependent only on the shape of the Λ matrix) is a minimum. This is a variational problem which, according to the authors of Ref. [35], should be solved numerically. The final result they expect to obtain is a value of near unity for α, which allows neglecting anisotropy.

The idea outlined above was implemented by the authors of Ref. [36], who succeeded in numerically finding the optimal transformation as programmed in Ref. [35]. The anisotropy factor was indeed found to be close to unity ($\alpha = 1.04$), so that the cloaking shell is considered in Ref. [36] as virtually isotropic, meaning that its refractive index is single and spatially inhomogeneous.

Figure 23 shows the distribution of this index throughout the cloaking layer. Importantly, the refractive index is nowhere less than unity, which essentially means the implementation of the idea of cloaking in an optically dense medium. True, in this approach total invisibility is impossible without a matching layer.

Although there is now no need to satisfy the conditions $\varepsilon, \mu < 1$, the authors of Ref. [36] use metamaterials to create

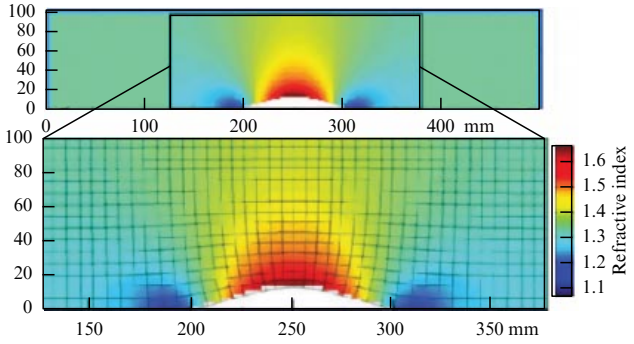

Figure 23. Refractive index distribution in a cloaking layer (taken from Ref. [36]).

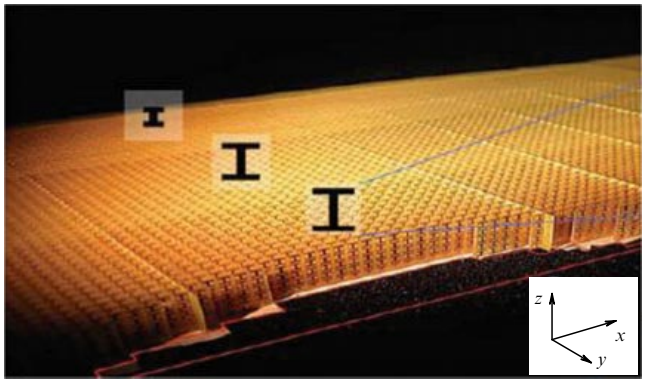

Figure 24. Cloaking layer structure (taken from Ref. [36]).

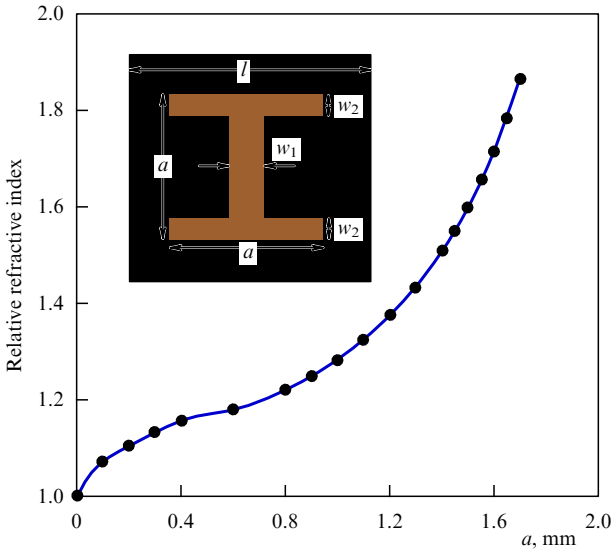

Figure 25. Geometric details of an I-element and its contribution to the refractive index (taken from Ref. [36]).

cloaking devices. This time, metamaterials consisting of I-shaped elements operate at frequencies *below* the resonant frequency (note that in most metamaterials $\varepsilon, \mu < 1$ for frequencies *above* the resonant one, whereas at low frequencies they also have $\varepsilon, \mu > 1$).

Reference [36] presents experimental results of plane layer cloaking. The cloaking layer they created consisted of about 10,000 I-elements, more than 6,000 of them being unique (Figs 24 and 25).

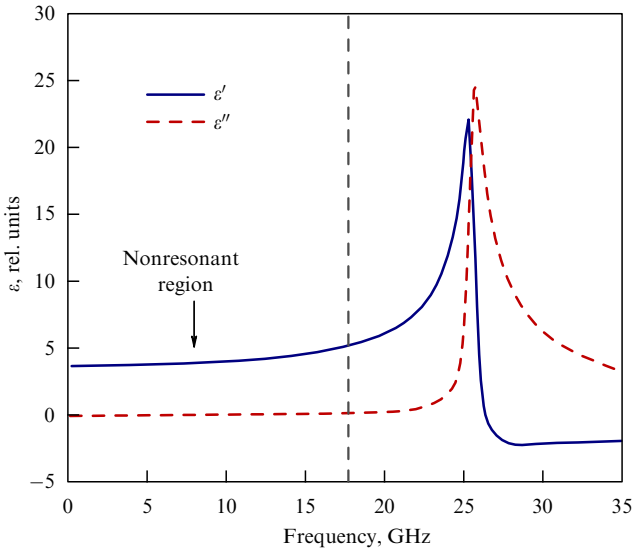

Figure 26. Approximate form of $\varepsilon(\omega)$ for an I-element (taken from Ref. [36]).

Through the efforts of the designers of this layer a special library of data on the refractive index and impedance as functions of size was compiled for metamaterials consisting of identical I-elements (it goes without saying that the data were obtained numerically). Using this library, a structure with the desired distributions of refractive index and impedance can be obtained. The location of each individual element (or 'metaatom') in this structure is not determined 'by hand', but is calculated with a simple Monte Carlo algorithm.

The I-shaped metaatom is not at all an accidental choice. If such a cloaking shell is made of, for example, ring resonators, then any effort to minimize anisotropy will be of no avail. Indeed, the aim of these efforts is to decrease dispersion, but ring resonators by themselves have considerable dispersion in the (near-resonance!) $\varepsilon, \mu > 1$ range.

Numerical experiments in Ref. [36] demonstrated that while I-shaped elements also have a resonant frequency, a frequency range (below the resonant frequency) where dispersion is virtually absent exists for them; this is the so-called nonresonant region (Fig. 26). The sizes of the I-elements were chosen so that their permittivities had the desired value precisely in the nonresonant frequency range. As a result, the metamaterial synthesized from these elements turned out to have negligible dispersion.

Thus, a cloaking shell with very low dispersion was obtained. In addition to lower absorption, one more great advantage here is that the cloaking effect is observed in a broader frequency range.

The experiments of Ref. [36] were carried out at four different frequencies: 13, 14, 15, and 16 GHz. Figure 27 presents the results of these experiments. The fact that the field patterns are virtually identical for all four frequencies allows the conclusion that the broadband cloaking effect does indeed show itself. The experimenters believe (but could not verify because of facility limitations) that this cloaking device has in fact a wider operation regime.

Thus, the plane cloaking layer solves a number of serious problems at one fell swoop:

- extension of the frequency range;
- a decrease in absorption;

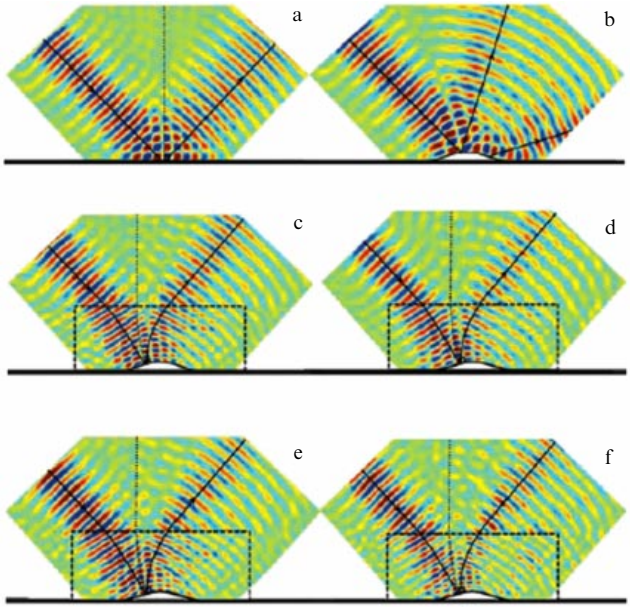

Figure 27. Oblique incidence of a ray on (a) a background surface (14 GHz), (b) an object (14 GHz), (c) a cloaked object (14 GHz), (d) a cloaked object (13 GHz), (e) a cloaked object (15 GHz), (f) a cloaked object (16 GHz) (taken from Ref. [36]).

• elimination of the singular point problem (the indentation in the layer 'grows' from a plane region underneath).

The fact that the layer is flat is not actually of fundamental significance: all the above listed problems were solved not in terms of shape but rather by minimizing anisotropy. It is hoped, therefore, that cloaks of more complex shapes but with the same remarkable properties will be developed in the near future.

9. Some practical problems in cloaking

The plane cloaking experiment of Ref. [36] allows the assertion that coordinate transformations can *in principle* produce an almost perfect cloaking effect. However, it is so far the only experiment of this kind, not counting the first cylindrical shell experiments [2] which were conducted under, shall we say, hothouse laboratory conditions: the incident radiation — planar; the surrounding medium — homogeneous, and the object cloaked — passive.

All this is irrelevant to our practical purposes. Given a typical applied problem — say, to make invisible a missile flying in the air at 2 km s^{-1} in the frequency range of 1–5 GHz — new questions immediately arise.

• A moving object always scatters differently than when at rest. Does motion affect the invisibility properties of an object (via the Doppler effect, for example)?

• The air, and even more so the exhaust wake, can be rather inhomogeneous. Can the ambient inhomogeneity be taken into account beforehand when designing the cloaking device?

• A missile (if of course it is a controlled one, as most current missiles are) should receive and transmit signals. But an object placed within a cloak becomes blind! If anything, it cannot receive signals in the cloaking range (which simply cannot penetrate to the interior), and indeed a signal in another frequency ranges can be scattered in a totally unpredictable way in the cloak.

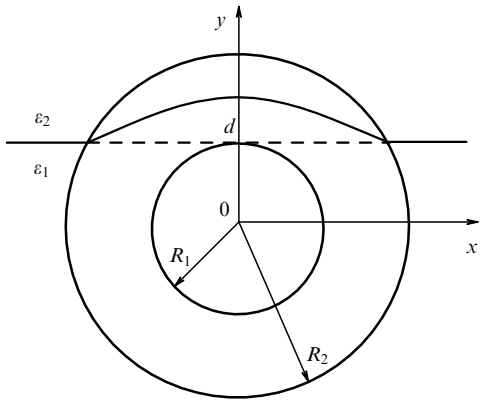

Figure 28. Cylindrical cloaking shell in a double layer medium (taken from Ref. [38]).

Such are the problems that stick out, but how many more are going to emerge when the cloaking of a real-life missile is attempted!

The above problems have, of course, been long recognized, and the first proposals for solving them have already appeared. We intend now to consider these.

9.1 Ambient inhomogeneity

The coordinate transformation method allows for cloaking in an inhomogeneous and even anisotropic surrounding medium (although the $\hat{\varepsilon}$ and $\hat{\mu}$ tensors of the cloaking shell were originally derived for an isotropic surrounding medium (see Appendix I), the extension to the anisotropic case is straightforward [37]). However, the more complex the properties of the surrounding medium, the more complex those of the cloak.

Consider, as an example, the results concerning a cylindrical cloaking shell in a double layer medium [38]. Figure 28 depicts the parameters of the problem. The results for the permittivity and permeability components have the form (7) but (the only difference) with all components of the $\hat{\varepsilon}$ tensor multiplied by the expression $\varepsilon_1 \operatorname{sign}(d - r\sin\varphi) + \varepsilon_2 \operatorname{sign}(r\sin\varphi - d)$. Thus, the permittivity of the shell is nonuniform not only in r but also in φ, and all its components depend on the layer permittivities ε_1 and ε_2 and the position of the interface d. It is clear that displacing the cloaking shell with respect to the interface strongly distorts the cloaking effect.

This approach requires prior knowledge of the distribution of ambient refractive index, and the cloaking effect will occur only for a certain position of the shell with respect to its surroundings. This inflexibility implies that such a cloak will hardly meet the practical requirements, i.e., the cloaking problem in an inhomogeneous medium remains open.

9.2 Blindness of the object being cloaked

In many practical cases cloaking does indeed turn out to be of no use if it prevents the object cloaked from communicating with the world outside. The most obvious way out is to make a shell with a 'window' in it. But how to prevent the window from hampering the cloaking effect?

One proposal [39] consists in creating a cylindrical shell in the form of a variable thickness layer (Fig. 29) such that at its narrowest cross section the permittivity and permeability tensors of the shell and of the environment are approxi-

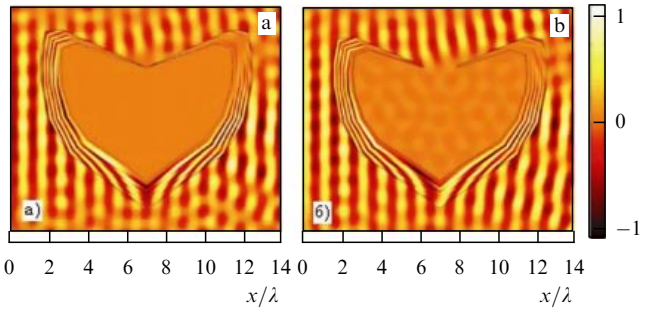

Figure 29. Normalized amplitude distribution for the electric field of radiation incident on a closed (a) and open (b) heart-shaped cloaking shell (taken from Ref. [39]).

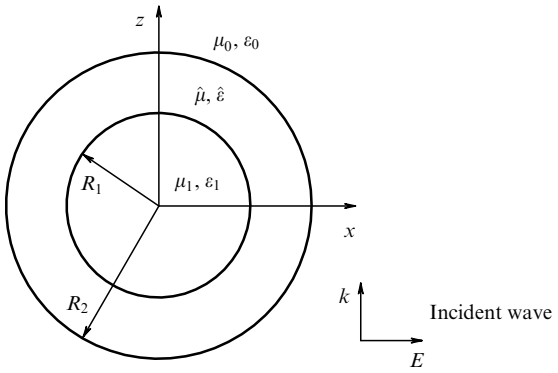

Figure 30. Spherical cloak (taken from Ref. [41]).

mately equal, $\varepsilon_{ij} \approx \varepsilon'_{ij}$, $\mu_{ij} \approx \mu'_{ij}$ (strict equality is generally impossible to achieve, while at the same time maintaining the ideal cloaking effect). This narrow region can then be removed without substantial damage, resulting in a window.

Of course, the partial removal of the shell causes some distortion of the cloaking effect — to a degree which depends on how much the components of the $\hat{\varepsilon}$ and $\hat{\varepsilon}'$ ($\hat{\mu}$ and $\hat{\mu}'$) tensors will ultimately differ in the window region. For example, a hole in a simple spherical cloak will produce much stronger distortion.

To find the corresponding transformation for such an open shell requires numerical work. The transformation is defined piecewise (using the polygon method), allowing even more than one window to be made.

10. Theoretical description of cloaking

The above discussion of achievements and challenges in the field of cloaking relied on numerical assumption–verification experiments. However, the researchers involved did not limit themselves to empirical studies (nor would their colleagues in any other field) and started developing theoretical models for describing cloaking by the wave flow method. Now what does it mean exactly to describe cloaking theoretically? The answer is, given the conditions of the problem (the type of the incident wave, and geometrical and material parameters of the shell), to derive analytical expressions for the electric and magnetic field components at any point at any time.

One possibility is, of course, to substitute the problem parameters into the system of Maxwell's equation and, having solved it, to obtain exact values for the components of the **B** and **D** vectors. The problem is only that, except for some simple cases, Maxwell's equations are not solved analytically. Cloaking problems are, due primarily to their anisotropy, too complicated for this, which leaves numerical methods as the only tool for directly solving Maxwell's equations.

The theoretical model of cloaking currently used by most researchers is based on the decomposition of the vectors **B** and **D** at every point into two mutually perpendicular components, each considered independent (according to the Mie theory of light scattering, this is legitimate in the absence of field sources). The reader is referred to Ref. [40] for a general exposition of this model. Let us consider this model as applied to the spherical cloaking shell discussed in Ref. [41].

Suppose a cloaked sphere is exposed to a z-directed linearly polarized electromagnetic wave (Fig. 30), so that $\mathbf{E} = \mathbf{e}_\mathbf{x} \exp(\mathrm{i}k_0 z)$, where $k_0 = \omega\sqrt{\mu_0\varepsilon_0}$ is the free-space wave vector. The time-dependent factor $\exp(-\mathrm{i}\omega t)$ will be omitted throughout.

It can be shown that electromagnetic field vectors can at any point be represented as two mutually perpendicular components, to each of which its own vector potential corresponds:

$$\mathbf{B}_{\mathrm{TM}} = \nabla \times \mathbf{A}_{\mathrm{TM}}\,, \tag{30a}$$

$$\mathbf{D}_{\mathrm{TM}} = \frac{\mathrm{i}}{\omega}\left\{\nabla \times [\hat{\mu}^{-1}\nabla \times \mathbf{A}_{\mathrm{TM}}]\right\}, \tag{30b}$$

$$\mathbf{B}_{\mathrm{TE}} = \frac{\mathrm{i}}{\omega}\left\{\nabla \times [\hat{\varepsilon}^{-1}\nabla \times \mathbf{A}_{\mathrm{TE}}]\right\}, \tag{30c}$$

$$\mathbf{D}_{\mathrm{TE}} = -\nabla \times \mathbf{A}_{\mathrm{TE}}\,. \tag{30d}$$

Subscript TM corresponds to the TM mode with respect to the vector **r**: $\mathbf{B}_{\mathrm{TM}} \perp \mathbf{r}$, $\mathbf{D}_{\mathrm{TM}} \parallel \mathbf{r}$, and subscript TE corresponds to the TE mode with respect to the vector **r**: $\mathbf{D}_{\mathrm{TE}} \perp \mathbf{r}$, $\mathbf{B}_{\mathrm{TE}} \parallel \mathbf{r}$.

For example, for the incidence direction shown in Fig. 30, the incident wave at point $(R_2, 0, 0)$ resides in the form of a TM mode: $\mathbf{D}_{\mathrm{TM}} = \varepsilon_0\mathbf{E}$, $\mathbf{B}_{\mathrm{TM}} = \mu_0\mathbf{H}$ ($\mathbf{D}_{\mathrm{TE}} = 0$, $\mathbf{B}_{\mathrm{TE}} = 0$). At point $(0, 0, R_2)$, on the contrary, there is only a TE mode: $\mathbf{D}_{\mathrm{TE}} = \varepsilon_0\mathbf{E}$, $\mathbf{B}_{\mathrm{TE}} = \mu_0\mathbf{H}$ ($\mathbf{D}_{\mathrm{TM}} = 0$, $\mathbf{B}_{\mathrm{TM}} = 0$). At other points, both regimes are present and $\mathbf{D} = \mathbf{D}_{\mathrm{TE}} + \mathbf{D}_{\mathrm{TM}}$, $\mathbf{B} = \mathbf{B}_{\mathrm{TE}} + \mathbf{B}_{\mathrm{TM}}$.

The vector potentials $\mathbf{A}_{\mathrm{TE}}$ and $\mathbf{A}_{\mathrm{TM}}$ corresponding to the TE and TM modes are at each point parallel to vector **r** (because it is with respect to vector **r** that we have decomposed the field into the TM and TE components), so that they can be represented in the forms

$$\mathbf{A}_{\mathrm{TE}} = \mathbf{e}_\mathbf{r}\Phi_{\mathrm{TE}}\,, \qquad \mathbf{A}_{\mathrm{TM}} = \mathbf{e}_\mathbf{r}\Phi_{\mathrm{TM}}\,, \tag{31}$$

where Φ_{TM} and Φ_{TE} are the so-called scalar potentials (not to be confused with the electrostatic potential).

In expressions (30) $\hat{\varepsilon}$ and $\hat{\mu}$ are the permittivity and permeability tensors of the shell, with components given by expressions (4). Because $\varepsilon_{\theta\theta} = \varepsilon_{\phi\phi}$, we will use the same symbol ε_t for both and, similarly, $\mu_{\theta\theta} = \mu_{\phi\phi} = \mu_\mathrm{t}$.

From Eqns (30) and (31) we find the wave equation for Φ_{TE} and Φ_{TM} giving, in spherical coordinates, the following:

$$\left[\frac{1}{\mathrm{SR}}\frac{\partial^2}{\partial r^2} + \frac{1}{r^2\sin\theta}\frac{\partial}{\partial\theta}\left(\sin\theta\,\frac{\partial}{\partial\theta}\right) + \frac{1}{r^2\sin^2\theta}\frac{\partial^2}{\partial\varphi^2} + \frac{1}{\mathrm{SR}}\,k_\mathrm{t}^2\right]\Phi = 0\,, \tag{32}$$

where $k_t = \omega\sqrt{\varepsilon_t\mu_t}$, and where $SR = \varepsilon_t/\varepsilon_{rr}$ for the TM component, and $SR = \mu_t/\mu_{rr}$ for the TE component.

Equation (32) is solved by the standard method of separation of variables. Putting $\Phi = f(r)\,g(\theta)\,h(\varphi)$ we obtain $h(\varphi) = \exp(\pm im\varphi)$ (harmonic functions), $g(\theta) = P_n^m(\cos\theta)$ (associated Legendre polynomials), and $f(r) = k_t(r - R_1)\,b_n[k_t(r - R_1)]$, where b_n are spherical Bessel functions.

The solutions so obtained can be written out as

$$\begin{aligned}\Phi^c_{TM} &= \frac{\cos\varphi}{\omega}\sum_n\Big\{d_n^{(M)}\psi_n\big[k_t(r-R_1)\big] \\ &\quad + f_n^{(M)}\chi_n\big[k_t(r-R_1)\big]\Big\}P_n^1(\cos\theta)\,, \\ \Phi^c_{TE} &= \frac{\sin\varphi}{\omega\eta_0}\sum_n\Big\{d_n^{(N)}\psi_n\big[k_t(r-R_1)\big] \\ &\quad + f_n^{(N)}\chi_n\big[k_t(r-R_1)\big]\Big\}P_n^1(\cos\theta)\,.\end{aligned} \tag{33}$$

Here, $d_n^{(M)}$, $d_n^{(N)}$, $f_n^{(M)}$, and $f_n^{(N)}$ are the unknown expansion coefficients, $\psi_n(\xi)$ and $\chi_n(\xi)$ are Riccati–Bessel functions of the first and second kind, and $\eta_0 = \sqrt{\mu_0/\varepsilon_0}$, $n = 1, 2, 3, \ldots$. Scalar potentials are marked by 'c' for cloak, indicating that the solutions are obtained for the interior of the cloak, i.e., $R_1 < r < R_2$.

This is now to be followed by matching the solutions with the scalar potentials of the incident (i) and scattered (s) radiation for $r > R_2$ and the internal ('in') field within the cavity of the cloak, i.e., for $r < R_1$. This is conveniently done by representing these potentials in terms of spherical harmonics:

$$\begin{aligned}\Phi^i_{TM} &= \frac{\cos\varphi}{\omega}\sum_n a_n\psi_n(k_0 r)\,P_n^1(\cos\theta)\,, \\ \Phi^i_{TE} &= \frac{\sin\varphi}{\omega\eta_0}\sum_n a_n\psi_n(k_0 r)\,P_n^1(\cos\theta)\,,\end{aligned} \tag{34}$$

$$\begin{aligned}\Phi^s_{TM} &= \frac{\cos\varphi}{\omega}\sum_n a_n T_n^{(M)}\zeta_n(k_0 r)\,P_n^1(\cos\theta)\,, \\ \Phi^s_{TE} &= \frac{\sin\varphi}{\omega\eta_0}\sum_n a_n T_n^{(N)}\zeta_n(k_0 r)\,P_n^1(\cos\theta)\,,\end{aligned} \tag{35}$$

$$\begin{aligned}\Phi^{in}_{TM} &= \frac{\cos\varphi}{\omega}\sum_n c_n^{(M)}\psi_n(k_1 r)\,P_n^1(\cos\theta)\,, \\ \Phi^{in}_{TE} &= \frac{\sin\varphi}{\omega\eta_0}\sum_n c_n^{(N)}\psi_n(k_1 r)\,P_n^1(\cos\theta)\,.\end{aligned} \tag{36}$$

Here, $a_n = (-i)^{-n}(2n+1)/[n(n+1)]$, $c_n^{(M)}$, $c_n^{(N)}$, $T_n^{(M)}$, and $T_n^{(N)}$ are the expansion coefficients, $\zeta_n(\xi)$ is the Riccati–Bessel function of the third kind, and $k_1 = \omega\sqrt{\varepsilon_1\mu_1}$.

From the matching conditions at the boundaries $r = R_1$ and $r = R_2$ (the continuity of the potentials and of their first derivatives), it can be seen that some of the expansion coefficients should be identically zero. These are $c_n^{(M)}$, $c_n^{(N)}$, $T_n^{(M)}$, $T_n^{(N)}$, $f_n^{(M)}$, and $f_n^{(N)}$. Thus, we arrive at the conclusion that fields are absent in the cavity of the cloak (as are stray fields). This is exactly what corresponds to the perfect cloaking effect.

Substituting expressions for scalar potentials first into Eqn (60) and then into Eqn (59), it is an easy matter to obtain analytical expressions for the components of the **B** and **D** vectors at any point in space.

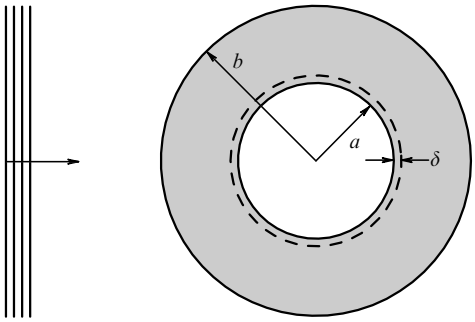

Figure 31. Cylindrical cloak with perturbation δ (taken from Ref. [42]).

The same procedure can be carried out for any shape of cloaking shell: it is only necessary that all the problem parameters be first expressed in spherical coordinates. If, as is sometimes the case, a coordinate system conformal to the shape of the shell is more convenient to work with, then Φ^i, Φ^s, and Φ^{in} should be represented as series expansions in special functions suited to the geometry of the problem, rather than in spherical functions. This was done, for example, in Ref. [42], which performs a theoretical analysis of a cylindrical cloak with the parameters (7) and in which all the potentials are expanded in cylindrical (Bessel, Hankel, or Neumann) functions. There is one more point to note: in the cylindrical problem, the decomposition of the fields into TE and TM components is with respect to the cylinder axis, not the radius vector.

Theoretical analysis has revealed a number of interesting features in the behavior of cloaking shells. The same Ref. [42], for example, analyzed a nonperfect cylindrical shell without a thin inner layer δ (Fig. 31). The tensor components $\varepsilon_{\phi\phi} = \mu_{\phi\phi} = r/(r-a)$ on the inner surface of the cylindrical cloak became infinite, and the authors of Ref. [42] set to check, with the view to avoid singular points, how strongly the removal of the thin inner layer influences the cloaking effect.

Using the above theoretical model, they wrote down the amplitude of the radiation scattered by a δ-perturbed shell. Letting δ tend to zero, they found that when δ is decreased by three orders of magnitude, scattering amplitude decreases at most by one! Such slow convergence implies that even the slightest deviation from the perfect shape will cause significant scattering, which undoubtedly makes the cylindrical shell with parameters (7) ineffective. It is, in fact, this study which encouraged the search for cylindrical shells free of singular points (see Section 7).

The same theoretical model has been applied to describe the interaction of cloaking shells with spherical and cylindrical waves [43, 44] (recall that all the previously mentioned studies assumed incident radiation to have a plane front). It was revealed that cloaking devices with perfect parameter values maintain their cloaking properties for spherical and cylindrical electromagnetic waves.

Finally, this theory was instrumental in finding new applications for the method of coordinate transformation. The authors of Ref. [40] found that by varying the form of the transformation for a spherical shell, it is possible to obtain a concentrator or rotator of an electromagnetic field instead of a cloaking device (Fig. 32).

It should be noted that solutions (33) were obtained for particular forms of the permittivity and permeability tensors.

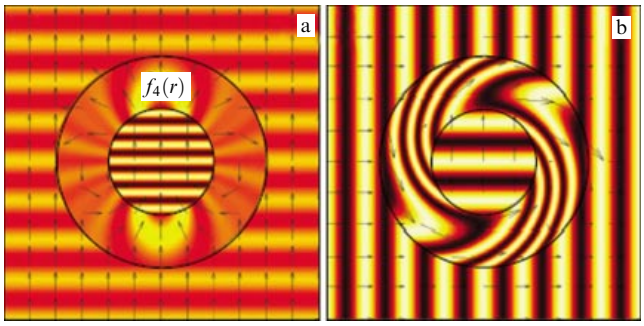

Figure 32. Concentrator and rotator interacting with an electromagnetic field: (a) electric field amplitude distribution for incidence on a field concentrator, and (b) magnetic field amplitude distribution for incidence on a field rotator (dark arrows indicate the direction of the Poynting vector). (Taken from Ref. [40].)

Were these tensors represented in the general form [through the transformation functions $r' = f(r, \theta, \varphi)$, $\theta' = g(r, \theta, \varphi)$, $\varphi' = h(r, \theta, \varphi)$], the expressions for the scalar potentials would be more complicated. To give an example, here is the general expression obtained in Ref. [40]:

$$\Phi = \hat{B}_n(k_0 f)\, P_n^m(\cos g)(A_m \cos mh + B_m \sin mh)\,, \qquad (37)$$

where $\hat{B}_n(\xi)$ is the Riccati–Bessel function, and A_m and B_m are unknown expansion coefficients.

Because expression (37) for the scalar potential directly involves transformation functions, these will also enter the final expressions for the electric and magnetic field vectors. Thus, by varying the form of coordinate transformation, a desired field configuration can be achieved. This is exactly the way in which the transformations that yield the concentrator and rotator of an electromagnetic field were obtained. In the former case, this is a linear transformation: $r' = cr + d$, $\theta' = \theta$, $\varphi' = \varphi$, and only the boundary conditions are different from those for the cloaking shell. In the latter case, this is the logarithmic transformation: $r' = r$, $\theta' = \theta$, $\varphi' = \varphi_0[(\ln r - \ln R_2)/(\ln R_1 - \ln R_2)]$.

11. Beyond electrodynamics

Maxwell's equations describing electromagnetic waves are invariant under space transformations, and it is exactly this fact which lies at the heart of the cloaking method we are discussing. Now, besides electromagnetic waves, other types of waves also exist, such as elastic, plasma, gravitational, probability density, etc., each of which is described by equations that have wave type solutions. If these equations are also invariant under coordinate transformations, then all the ideas we discussed in Section 3 for electromagnetic waves are applicable to other types of waves.

11.1 Acoustic cloaking

The fact, shown in Ref. [45], that elastic wave equations possess this invariance property impacted the development of acoustic cloaking, which is the full analogue of its electromagnetic counterpart. The role of the permittivity and permeability tensors is here played by the mass density tensor.

Although a material with anisotropic density seems at first sight rather exotic, the model demonstrated in Fig. 33 clearly illustrates that such media can be created. If the vertical and

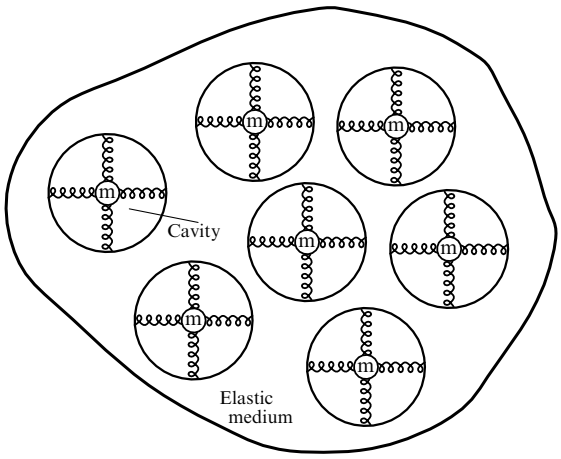

Figure 33. Medium with an anisotropic mass density. Horizontal and vertical strings have different stiffnesses; at the center of each cavity is a load of mass m attached to the strings (taken from Ref. [45]).

horizontal strings differ in stiffness, the properties of such a medium will be different in different directions, which makes the medium anisotropic.

The density tensor for an acoustic cloaking shell is readily obtained based on the parameters of its electromagnetic analogue [46]. Note first that the continuity equation which follows from Maxwell's equations has the form

$$\nabla\big[\sigma(x)\nabla V(x)\big] = f(x)\,, \qquad (38)$$

where $V(x)$ is the electric potential, $\sigma(x)$ is the conductivity, and $f(x)$ is the source function.

A similar equation, also following from momentum conservation law and the stress–strain relationship, can be written out for sound vibrations in the form

$$\nabla\left[\frac{1}{\rho(x)}\,\nabla p(x)\right] = -\frac{\omega^2}{\lambda(x)}\,p(x)\,, \qquad (39)$$

where $\rho(x)$ is the density, $p(x)$ is the pressure, $\lambda(x)$ is the elasticity modulus, and ω is the vibration frequency.

Note here the correspondence

$$\big[V(x), \sigma(x), f(x)\big] \leftrightarrow \left[p(x)\,, \frac{1}{\rho(x)}\,, -\frac{\omega^2}{\lambda(x)}\,p(x)\right]. \qquad (40)$$

In an electromagnetic field, the transformation $(x_1, x_2, x_3) \to (x_1', x_2', x_3')$ with the matrix A $(A_{ki} = \partial x_k'/\partial x_i)$ yields

$$\hat{\sigma}'(x') = \frac{A\sigma(x)A^{\mathrm{T}}}{\det A}\,, \qquad (41)$$

$$f'(x') = \frac{f(x)}{\det A}\,, \qquad (42)$$

where $\hat{\sigma}'(x')$ this time is the conductivity tensor. Then from correspondence (40), one finds $1/[\hat{\rho}'(x')] = A[1/\rho(x)]A^{\mathrm{T}}/\det A$ and $\lambda'(x') = \lambda(x)/\det A$. For example, using transformation (1) for a spherical shell we obtain

$$\rho'_{rr} = \frac{R_2 - R_1}{R_2}\,\frac{r'^2}{(r' - R_1)^2}\,, \qquad \rho'_{\theta\theta} = \rho'_{\phi\phi} = \frac{R_2 - R_1}{R_2}\,, \qquad (43)$$

$$\lambda'(r) = \frac{(R_2 - R_1)^3}{R_2^3}\,\frac{r'^2}{(r' - R_1)^2}\,. \qquad (44)$$

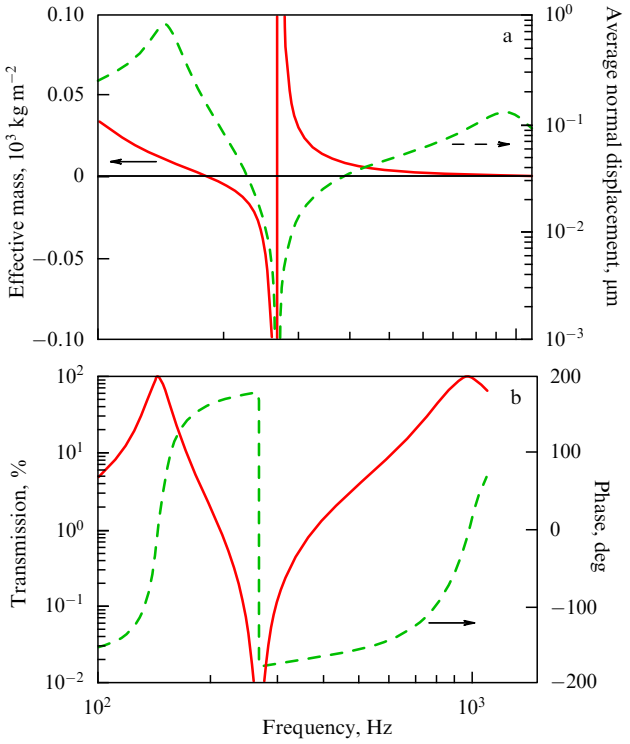

Figure 34. Characteristics of a resonator in the form of a thin finite-mass membrane: (a) effective mass (solid lines, left axis) and normalized vibration amplitude (dashed line, right axis), and (b) amplitude (solid line, left axis) and phase (dashed line, right axis) of a transmitted wave (taken from Ref. [47]).

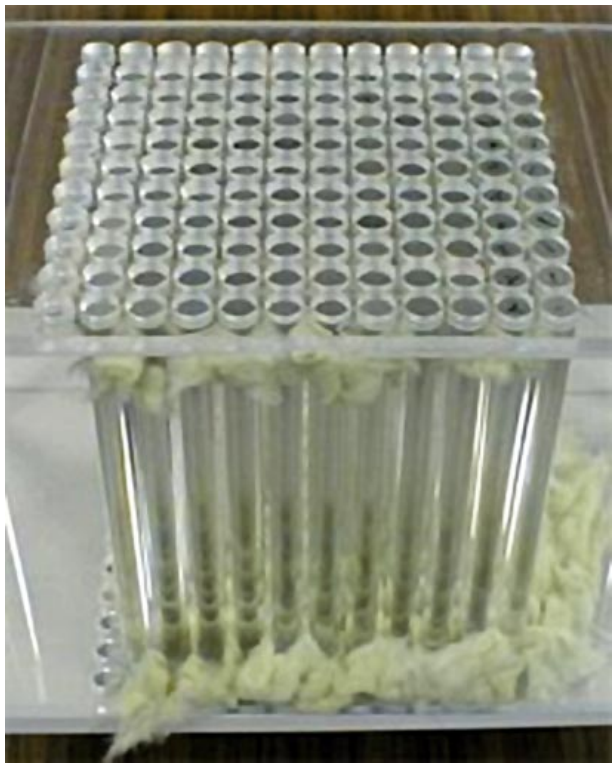

Figure 35. Prototype of acoustic material (from T Miyashita et al., in *Proc. 5th World Congress on Ultrasonics*; TO-PM04.02).

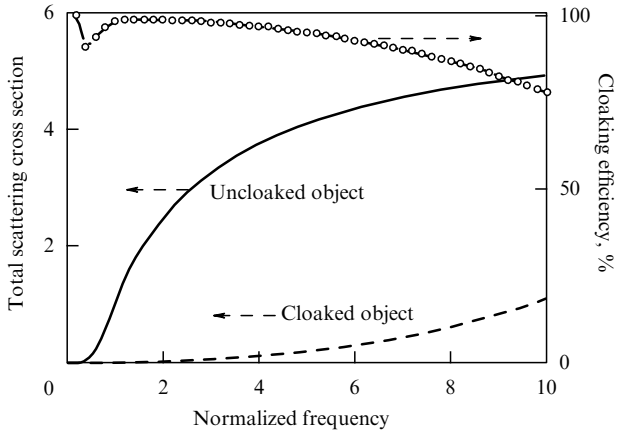

Figure 36. Total acoustic scattering cross section as a function of frequency: solid line corresponds to an uncloaked object, and the dashed line to a multilayer-cloaked one. The circles show cloaking efficiency (taken from Ref. [48]).

Such a cloak can be designed from acoustic metamaterials, which are also analogues of electromagnetic materials and which are composite media in the sense of an isotropic matrix with a periodic array of inclusions ('metaatoms'). Possible inclusions are strings, finite mass membranes, or structures similar to those shown in Fig. 33. Close to a resonant frequency, the effective mass of an individual resonator (for example, a membrane) can take negative values; however, similar to electromagnetic metamaterials, this is also the region of maximum absorption (Fig. 34) [47]. In yet another example, shown in Fig. 35, the acoustic metamaterial consists of a system of hollow cylinders placed within the thickness of a polymer material.

Many shapes of cloaking devices, including spherical, do not require that the material parameters be negative. However, in the electromagnetic case, to achieve values of $0 < \varepsilon, \mu < 1$ one needs inherently anisotropic metamaterials, because in usual dielectrics $\varepsilon, \mu > 1$. As for the density, among natural media one can find those with virtually any positive value of density. Therefore, the perfect acoustic coating can be approximately replaced by a multilayer coating consisting of several layers of an isotropic substance. The thickness of each layer should be much less than the incident wavelength, which presents no difficulty for sound waves.

As shown in Ref. [48], a multilayer (20 layers) acoustic coating gives a good cloaking effect. Because layers are in this case isotropic, the cloaking effect occurs over a fairly broad frequency range (Fig. 36). Thus, compared to the electromagnetic case, in the acoustic case the frequency range allowing for the cloaking effect is easier to extend.

11.2 Quantum-mechanical cloaking

Invariance in relation to coordinate transformations can also be proved for the stationary Schrödinger equation [49, 50]. When subjected to the transformation $(x_1, x_2, x_3) \to (q_1, q_2, q_3)$, the stationary Schrödinger equation with the effective mass tensor, written in paper [49], viz.

$$-\frac{\hbar^2}{2}\,\nabla\left[(\hat{m}^*)^{-1}\nabla\psi\right] + V(\mathbf{r})\psi = E\psi\,, \qquad (45)$$

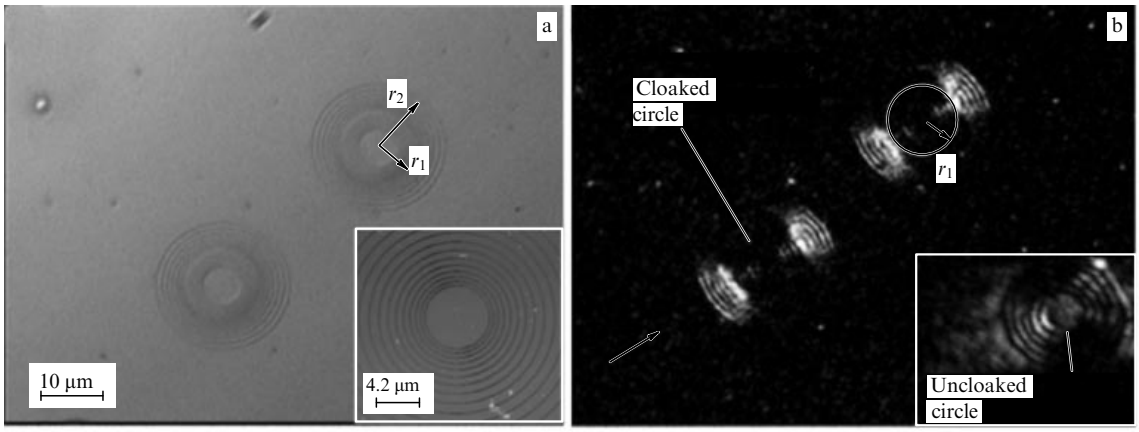

Figure 37. Microphotographs of ring microstructures: (a) white light illumination, and (b) surface plasmon cloaking at $\lambda = 532$ nm (taken from Ref. [57]).

retains its form if we set

$$\hat{m}' = \frac{\hat{h}\hat{m}\hat{h}}{|\det \hat{h}|}\,, \tag{46}$$

$$V' = E + |\det \hat{h}|\,(V - E)\,, \tag{47}$$

where $\hat{m}^* = m_0\hat{m}$ is the effective mass tensor, and $\hat{h}_{ij} = h_i\delta_{ij}$, $h_i = |\partial\mathbf{x}/\partial q_i|$ are the Lamé coefficients.

For example, performing the transformation $r' = g(r)$, $\theta' = \theta$, $\varphi' = \varphi$, the parameters for a spherical cloaking shell are found to be

$$V'(\mathbf{r}, E) = \left[1 - \left(\frac{g}{r}\right)^2 g'(r)\right] E\,, \tag{48}$$

$$m'_{rr} = g'(r)\left(\frac{r}{g}\right)^2 m_0\,, \qquad m'_{\theta\theta} = m'_{\phi\phi} = \frac{1}{g'(r)}\, m_0\,. \tag{49}$$

Thus, theoretically the cloaking method works as well for probability density waves; however, creating suitable media is still an open question. The first analogues of such media to be fabricated will most likely be semiconductor nanostructures.

11.3 Cloaking using wave type transformation

One further, very interesting, approach to cloaking is to change the type — or even the physical nature — of a wave propagating in the cloak. The idea is that the surface of a body is given certain properties (including impedance) at which the energy of the incident plane electromagnetic wave is mostly carried away by excited (secondary) waves of a different type, the remainder being absorbed by the surface. The secondary wave 'flows around' the body cloaked, is transformed back into an electromagnetic wave, reappears as light at the back side of the body and partially restores the form of the incident wave.

The secondary wave can be of various physical natures, including a surface electromagnetic wave (see Refs [51–53] for calculations) or a surface plasma wave (surface plasmons; see Refs [54, 55]). It should be remembered, though, that its phase velocity should exceed that of the primary wave for the phase front to be restored at the back side of the cloaked body. If the secondary wave is a surface wave, as considered in Refs [51–55], the wave transformation can allow for a much smaller thickness of the cloak. Moreover, secondary waves can be helpful in solving the problem of a blind cloaked object we mentioned in Section 9.2. Thus, Ref. [56] suggests and validates the idea of a sensor surrounded by a cloaking shell whose cloaking effect is obtained using a secondary wave (or plasmons): the sensor can receive, process, and transfer a signal while remaining invisible to the external observer. As a further advantage of a plasmon secondary wave, the cloaking of nanostructured objects in the optical range was demonstrated in Ref. [57] (see Fig. 37).

12. Related ideas

This section presents some new ideas that follow from, though have no direct relation to, the cloaking ideas discussed above. To better understand these ideas, let us here re-emphasize the key points of left-handed optics: plane [58] and spherical [59, 60] layers of left-handed material may possess the properties of a perfect lens; and it is possible to choose a coordinate transformation which allows a wave concentrator and a wave rotator to be built (see Fig. 32) [40]. The idea of a concentrator, when developed, leads, in principle, to highly directional antennas less than wavelength in size! As for the wave rotator, this is the first step to implementing the laboratory model of the black hole.

12.1 Small-sized directional antennas

There are two well-known traditional approaches to making highly directional antennas: using phased antenna arrays, and using quasioptical antennas (paraboloids, etc.) many wavelengths in size. Antennas around or even less than a wavelength in size produce poorly directional radiation, as exemplified by the hole-less-torus-shaped directional diagram of an elementary dipole.

Reference [61] demonstrated that, using a cloaking shell that implements a concentrator type coordinate transformation, it is possible to obtain a small-sized directional antenna. Shown in Fig. 38 are example results from wave pattern calculations performed in Ref. [61] for a plane, 8-cm-long, 2-GHz antenna surrounded by a shell with a radius of 20 cm. Similar calculations for a scaled-down parabolic antenna were performed in Ref. [62].

12.2 Laboratory black hole model

We have already noted in Section 3 that when implementing the cloaking by the wave flow method, there is a geometric equivalence between the way rays pass through the cloaking

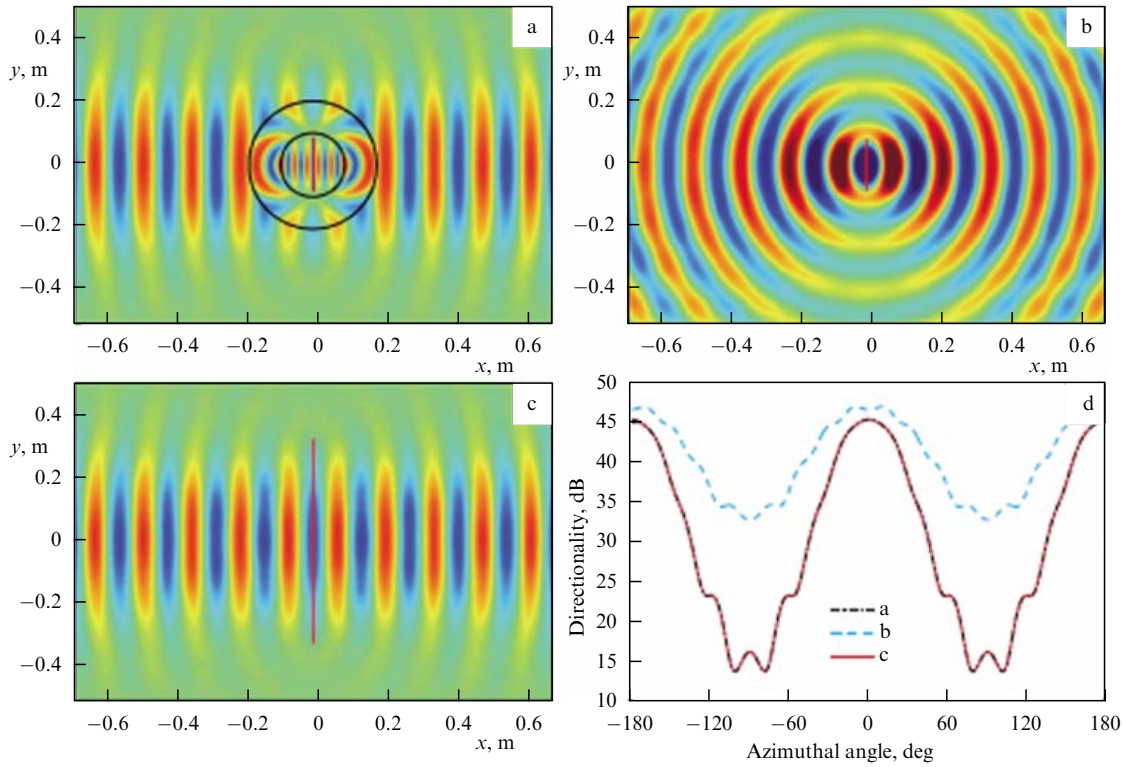

Figure 38. Calculated results for a small-sized highly directional antenna: (a) 8-cm-long antenna in a concentrating shell with outer and inner radii of 20 cm and 10 cm, respectively; (b) the same antenna uncloaked; (c) equivalent 32-cm-long antenna of the same directionality, and (d) directional patterns (taken from Ref. [61]).

Figure 39. Well-meant caricature of Albert Einstein highlighting mathematical equivalence between cloaking and antigravitation (taken from Ref. [63]).

material and the coordinate lines (and metric) under the conditions of antigravitation, with geodesic lines pushed apart. In Fig. 39, a caricature borrowed from Ref. [63] is given as an illustration. Such 'antigravitation' in a shell is, of course, virtual, with no chance of a massive particle being deflected.

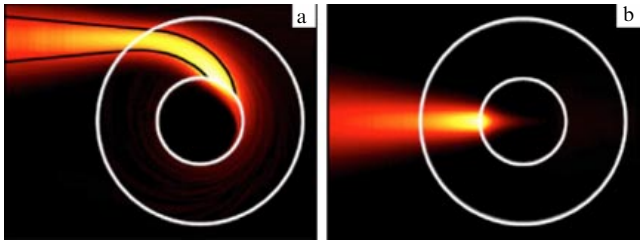

Figure 40. Calculated results for the capture of a Gaussian beam by a shell modeling a black hole: (a) lateral capture (black lines are for ray trajectories), and (b) central capture (taken from Ref. [64]).

Now, is it possible to model the deflection of an electromagnetic wave in a gravitational field, when the coordinate lines, on the contrary, come closer together? The answer turns out to be yes if one makes use of a coordinate transformation of the 'rotator' type. Figure 40 presents the results of calculating the capture of a wave by a cloaking shell discussed in Ref. [64]. The same wave capture is predicted by the general theory of relativity (GTR) for the neighborhood of a massive black hole: at whatever angles rays enter the shell they accumulate and are absorbed near the virtual 'horizon line'. Thus, an operating laboratory model of a black hole can become a prototype of a new generation of a solar heating cell with an absorption efficiency of close to 100%. Also, using such a capsule in laser-controlled fusion is worth considering in the very near future.

12.3 Wormhole and magnetic monopole models

In Ref. [65], a simple wormhole configuration was suggested as a development of the bulk models of gravitating objects in

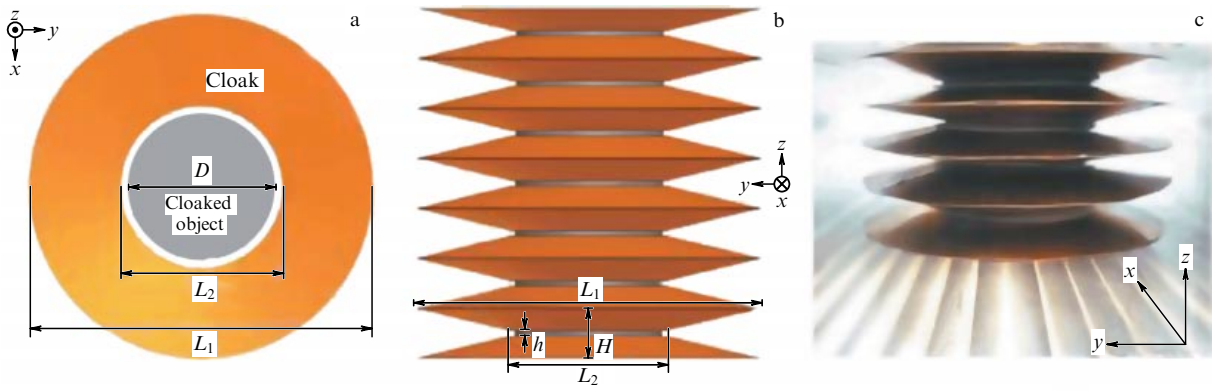

Figure 41. Geometry of a broadband microwave warped layered cloak [68]. Dimensions are as follows: $L_1 = 70$ mm, $L_2 = 32$ mm, $H = 9.2$ mm, $h = 1$ mm, $D = 30$ mm; the structure is placed in a rectangular waveguide (length × width × height = 432 × 86.36 × 36.8 mm): (a) top view, (b) front view, and (c) photograph.

GTR — a typical nontrivial metric structure which, for ordinary gravitation, allows for superluminal transport and even a so-called time machine [66, 67]. Its model uses a cylindrical cloaking tube and is applicable, of course, only to electromagnetic waves, not to massive particles. Its technological applications conceivably include new optical cables, optical computers, 3D video displays, and optical video systems for magnetic resonance visualization and so forth. One proposal is, curiously enough, an electromagnetic model of the monopole, also described in Ref. [65]. According to this model, the cloaking tube encloses the magnetic field lines between the opposite magnetic poles localized at the two ends of the tube.

The field of cloaking abounds with ideas. We see, at any rate, that a host of possibilities have opened up for synthesizing electromagnetic fields in networks containing tubular cloaking elements.

13. Recent experiments on wave flow cloaking

With new ideas, calculations, and experiments being published on a weekly basis, wave flow cloaking technologies seem to have reached their apogee in terms of development rate. This section presents some new experimental data which were obtained in what we consider unusual geometric and instrumental settings and which reveal new aspects in the method under review.

13.1 Broadband invisibility for a warped cylindrical scatterer in a waveguide

Experiments in Ref. [68] investigated a cylinder-shaped metallic object surrounded by a warped cloaking shell and placed in a rectangular waveguide. The shell was a set of truncated-cone-shaped metallic plates that were put on the cylinder. The geometry and design dimensions of these experiments are displayed in Fig. 41. The result was that the cloaking shell near the cylinder worked as a periodic sequence (stack) of radial waveguides of variable thickness (from H to h). The excitation, in the master waveguide, of a wave with the electric field parallel to the cylinder axis produced the cloaking effect — in the sense that the wave restored its shape after bending around the scatterer — and, as Fig. 42 shows, there is a wide range of frequencies for which the effect is possible.

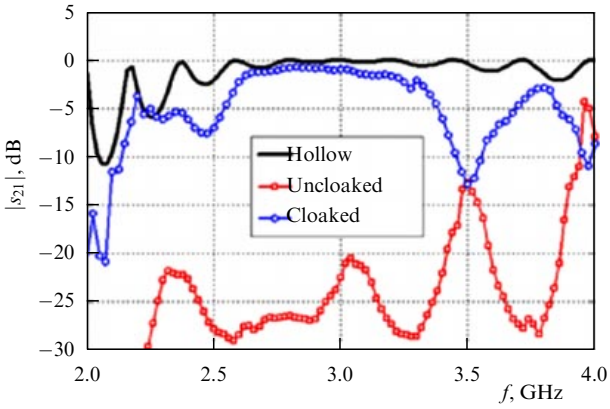

Figure 42. Waveguide transmission coefficient (from top to bottom: hollow waveguide, waveguide with an uncloaking shell, and waveguide with a cloaking shell) (taken from Ref. [68]).

13.2 Cloaking model using a lumped *LC* circuit

It is a well-known fact (see Ref. [69]) that an anisotropic dielectric medium with $\hat{\varepsilon}$ and $\hat{\mu}$ tensors can be represented as an equivalent electric circuit consisting of lumped *RLC* elements. In this circuit, the inductances L, capacitances C, and resistors R model the diagonal elements of the $\hat{\mu}$ tensor, the elements of the $\hat{\varepsilon}$ tensor, and dissipation, respectively, whereas the components of the electromagnetic field are equivalent to voltages and currents in the circuit elements.

Based on this simple idea, a circuit with lumped *LC* elements was used to experimentally model wave flow cloaking [70]. Specifically, a plane circular circuit (see Fig. 43) was assembled comprising 30 azimuthal layers with 90 microcircuits in each (15 inner and 15 outer layers modeling the cloaking shell and the background, respectively). Each of the microcircuits contained a cross-like assembly of four inductive elements, the center of the cross being grounded through a capacitor. The parameters of the *LC* elements were chosen so as to model the coordinate transformation (7).

The measured results are presented in Fig. 44. Notice the occurrence of a marked cloaking effect at three frequencies for a wave with a circular phase front.

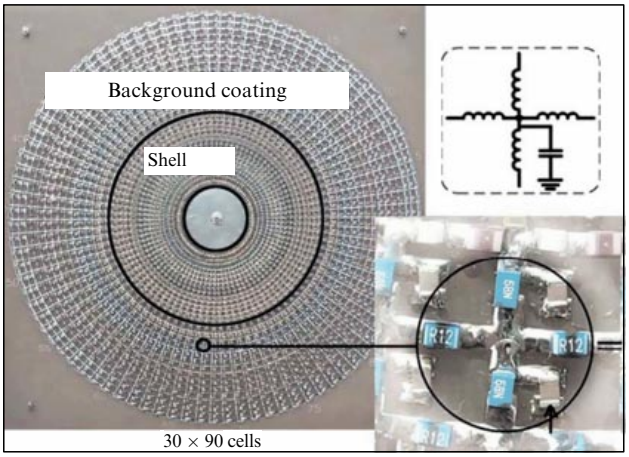

Figure 43. Photograph of an *LC* circuit modeling wave flow cloaking; upper right inset: equivalent circuit of the microdevice; lower inset: photograph of the microdevice (taken from Ref. [70]).

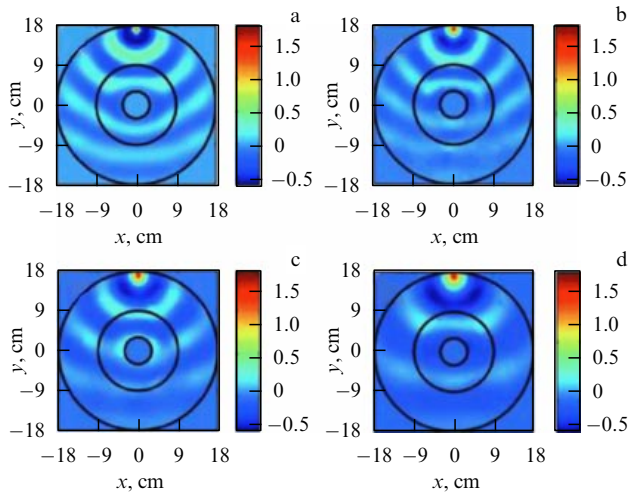

Figure 44. Investigation results of cloaking in an *LC* circuit: Panel a: calculations for a frequency of 40.1 MHz. Panels b, c, and d: measurements at 40.1 MHz, 32.0 MHz, and 24.0 MHz, respectively. (Taken from Ref. [70].)

14. Conclusion

This paper has outlined the theoretical background and basic ideas of wave flow cloaking. It is shown that the key mathematical problem in cloaking any particular object is to find the suitable spatial coordinate transformation on the basis of which expressions for the components of the permittivity and permeability tensors can be obtained.

The results obtained for cloaking shells of various shapes were presented. It was shown that the key problems in their design, such as extending the cloaking frequency range, decreasing anisotropy, securing the absence of magnetization, and eliminating the blindness of the cloaked object, and some others can be effectively solved by appropriately choosing the coordinate transformation.

The results of some series of experiments demonstrating the fundamental possibility of wave flow cloaking were presented.

15. Appendices

I. Proof of Maxwell's equations invariance under the general coordinate transformation

The proof follows Ref. [1].

Maxwell's equations in Cartesian coordinates are written out as

$$\nabla \times \mathbf{E} = -\mu\mu_0 \frac{\partial \mathbf{H}}{\partial t}\,, \qquad \nabla \times \mathbf{H} = +\varepsilon\varepsilon_0 \frac{\partial \mathbf{E}}{\partial t}\,, \tag{50}$$

where ε and μ are scalar functions of coordinates. Suppose the Cartesian coordinate system is subject to the nonsingular point transformation $q_1(x, y, z)$, $q_2(x, y, z)$, and $q_3(x, y, z)$. The intersections of the surfaces $q_2 = \text{const}$, $q_3 = \text{const}$ give coordinate lines q_1, etc. (Fig. 45), which are smooth due to the absence of singular points in the transformation.

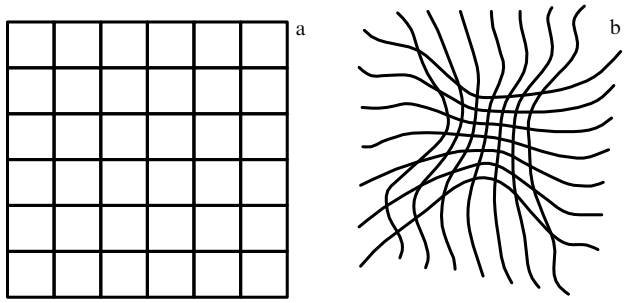

Figure 45. Coordinate grids (x, y, z) (a) and (q_1, q_2, q_3) (b) in the Cartesian coordinate system. (Taken from Ref. [1].)

Now, what will Maxwell's equation look like in the new coordinates?

Let $\mathbf{u}_1$, $\mathbf{u}_2$, and $\mathbf{u}_3$ be the unit vectors corresponding to the coordinate lines q_1, q_2, and q_3. The arc length element is given by

$$\begin{aligned} \mathrm{d}s^2 = \mathrm{d}x^2 + \mathrm{d}y^2 + \mathrm{d}z^2 = Q_{11}\,\mathrm{d}q_1^2 + Q_{22}\,\mathrm{d}q_2^2 + Q_{33}\,\mathrm{d}q_3^2 \\ + 2Q_{12}\,\mathrm{d}q_1\,\mathrm{d}q_2 + 2Q_{13}\,\mathrm{d}q_1\,\mathrm{d}q_3 + 2Q_{23}\,\mathrm{d}q_2\,\mathrm{d}q_3\,, \end{aligned} \tag{51}$$

where

$$Q_{ij} = \frac{\partial x}{\partial q_i}\frac{\partial x}{\partial q_j} + \frac{\partial y}{\partial q_i}\frac{\partial y}{\partial q_j} + \frac{\partial z}{\partial q_i}\frac{\partial z}{\partial q_j}\,. \tag{52}$$

The length element of the ith coordinate line is defined as

$$\mathrm{d}s_i = Q_i\,\mathrm{d}q_i\,, \tag{53}$$

where for brevity we denote

$$Q_i^2 = Q_{ii}\,. \tag{54}$$

To calculate $\nabla \times \mathbf{E}$, let us take a surface element small enough to be considered a parallelepiped (Fig. 46).

We now denote the projections of the $\mathbf{E}$ vector as

$$E_1 = \mathbf{E}\,\mathbf{u}_1\,, \quad E_2 = \mathbf{E}\,\mathbf{u}_2\,, \quad E_3 = \mathbf{E}\,\mathbf{u}_3 \tag{55}$$

and apply the Stokes theorem to obtain

$$\begin{aligned} &(\nabla \times \mathbf{E})(\mathbf{u}_1 \times \mathbf{u}_2)\,\mathrm{d}q_1\,Q_1\,\mathrm{d}q_2\,Q_2 \\ &\quad = \mathrm{d}q_1\,\frac{\partial}{\partial q_1}(E_2\,\mathrm{d}q_2\,Q_2) - \mathrm{d}q_2\,\frac{\partial}{\partial q_2}(E_1\,\mathrm{d}q_1\,Q_1)\,. \end{aligned} \tag{56}$$

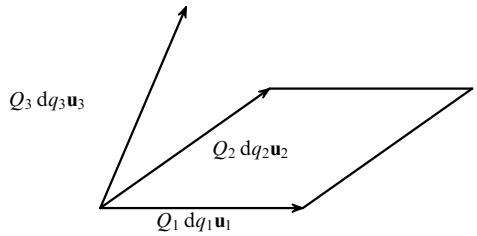

Figure 46. Parallelepiped built on vectors $\mathbf{u}_1$ and $\mathbf{u}_2$ is a small surface element. (Taken from Ref. [1].)

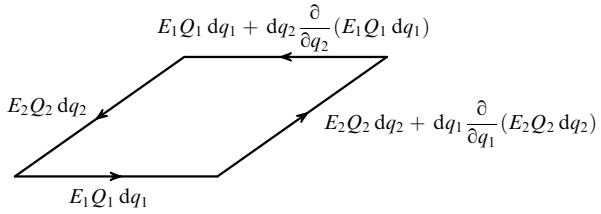

Figure 47. Integration contour for applying the Stokes theorem. (Taken from Ref. [1].)

The left-hand side of equation (56) is the flux of the curl of **E** through our surface element, whereas the right-hand side is a curvilinear integral over the contour of the parallelepiped (Fig. 47).

Dividing both parts of equation (56) by $\mathrm{d}q_1\,\mathrm{d}q_2$ yields

$$(\boldsymbol{\nabla}\times\mathbf{E})(\mathbf{u}_1\times\mathbf{u}_2)Q_1Q_2=\frac{\partial}{\partial q_1}\tilde{E}_2-\frac{\partial}{\partial q_2}\tilde{E}_1=(\boldsymbol{\nabla}_q\times\tilde{\mathbf{E}})^3\,, \quad (57)$$

where we have introduced

$$\tilde{E}_1=Q_1E_1\,,\quad \tilde{E}_2=Q_2E_2\,,\quad \text{and}\quad \tilde{E}_3=Q_3E_3\,. \quad (58)$$

The superscript 3 in Eqn (57) denotes the contravariant component of the vector $\boldsymbol{\nabla}_q\times\tilde{\mathbf{E}}$ (the curl of $\tilde{\mathbf{E}}$ in the new coordinates).

Let us write the magnetic field vector **H** in contravariant components:

$$\mathbf{H}=H^1\mathbf{u}_1+H^2\mathbf{u}_2+H^3\mathbf{u}_3\,. \quad (59)$$

Expression (59) can be recast in a covariant form by using the metric tensor g:

$$g^{-1}\begin{bmatrix}H^1\\H^2\\H^3\end{bmatrix}=\begin{bmatrix}\mathbf{u}_1\,\mathbf{u}_1 & \mathbf{u}_1\,\mathbf{u}_2 & \mathbf{u}_1\,\mathbf{u}_3\\ \mathbf{u}_2\,\mathbf{u}_1 & \mathbf{u}_2\,\mathbf{u}_2 & \mathbf{u}_2\,\mathbf{u}_3\\ \mathbf{u}_3\,\mathbf{u}_1 & \mathbf{u}_3\,\mathbf{u}_2 & \mathbf{u}_3\,\mathbf{u}_3\end{bmatrix}\begin{bmatrix}H^1\\H^2\\H^3\end{bmatrix}=\begin{bmatrix}H_1\\H_2\\H_3\end{bmatrix}, \quad (60)$$

or

$$H^i=\sum_{j=1}^{3}g^{ij}H_j\,. \quad (61)$$

Multiplying the right-hand and left-hand sides of Maxwell's equation $\boldsymbol{\nabla}\times\mathbf{E}=-\mu\mu_0\,\partial\mathbf{H}/\partial t$ by $(\mathbf{u}_1\times\mathbf{u}_2)Q_1Q_2$ and using Eqns (59) and (61) we obtain

$$\begin{aligned}(\boldsymbol{\nabla}\times\mathbf{E})(\mathbf{u}_1\times\mathbf{u}_2)Q_1Q_2&=\mu_0\mu\frac{\partial\mathbf{H}}{\partial t}(\mathbf{u}_1\times\mathbf{u}_2)Q_1Q_2\\&=-\mu_0\mu\sum_{j=1}^{3}g^{3j}\frac{\partial H_j}{\partial t}\,\mathbf{u}_3(\mathbf{u}_1\times\mathbf{u}_2)Q_1Q_2\,. \quad (62)\end{aligned}$$

Introducing the notation

$$\tilde{H}_j=Q_jH_j\,, \quad (63)$$

$$\mu^{ij}=\mu g^{ij}\big|\mathbf{u}_1(\mathbf{u}_2\times\mathbf{u}_3)\big|Q_1Q_2Q_3(Q_iQ_j)^{-1} \quad (64)$$

and using Eqns (64) and (57) we arrive at

$$(\boldsymbol{\nabla}_q\times\tilde{\mathbf{E}})^i=-\mu_0\sum_{j=1}^{3}\mu^{ij}\frac{\partial\tilde{H}_j}{\partial t}\,. \quad (65)$$

Taking into account the symmetry between the electric and magnetic fields, we can write down

$$(\boldsymbol{\nabla}_q\times\tilde{\mathbf{H}})^i=+\varepsilon_0\sum_{j=1}^{3}\varepsilon^{ij}\frac{\partial\tilde{E}_j}{\partial t}\,, \quad (66)$$

where

$$\varepsilon^{ij}=\varepsilon g^{ij}\big|\mathbf{u}_1(\mathbf{u}_2\times\mathbf{u}_3)\big|Q_1Q_2Q_3(Q_iQ_j)^{-1}\,. \quad (67)$$

Thus, Maxwell's equations (50) do retain their form under a transformation into coordinates (q_1,q_2,q_3).

II. Calculating ray trajectories in cloaking shells

Calculations below follow Ref. [71].

As known from geometrical optics, ray trajectories are defined by the equations

$$\frac{\mathrm{d}\mathbf{x}}{\mathrm{d}\tau}=\frac{\partial H}{\partial\mathbf{k}}\,, \quad (68)$$

$$\frac{\mathrm{d}\mathbf{k}}{\mathrm{d}\tau}=-\frac{\partial H}{\partial\mathbf{x}}\,. \quad (69)$$

Here, $\mathbf{x}=\{x,y,z\}$ is the radius vector in Cartesian coordinates, **k** is the wave vector, and τ is a parameter with a dimension of length. Hereinafter, $\partial f/\partial\mathbf{a}$ designates a vector with the components

$$\left\{\frac{\partial f}{\partial a_x}\,,\frac{\partial f}{\partial a_y}\,,\frac{\partial f}{\partial a_z}\right\}.$$

It can be shown [71] that the Hamiltonian H for an anisotropic medium with $\varepsilon=\mu=n$ assumes the form

$$H=f(\mathbf{x})(knk-\det n)\,, \quad (70)$$

with $f(\mathbf{x})$ being an arbitrary function of the radius vector.

A ray refracts twice when passing through a cloaking shell: at the entrance to and exit from it, and in either case boundary conditions must be satisfied. If the incident radiation is a plane wave, the boundary conditions have the form

$$(\mathbf{k}_1-\mathbf{k}_2)\times\boldsymbol{\nu}=0\,, \quad (71)$$

$$H(\mathbf{k}_2)=0\,, \quad (72)$$

where $\mathbf{k}_1$ and $\mathbf{k}_2$ are the wave vectors on one side and the other side of the interface, and $\boldsymbol{\nu}$ is the interface normal. Condition (71) expresses the continuity of the normal component of the **k** vector, and condition (72) is the requirement for the wave to maintain its front plane.

The set of equations (71) and (72) determines all components of the vector $\mathbf{k}_2$, but because the Hamiltonian is quadratic in **k**, this set has two solutions: one for energy

transfer from the first medium to the second, and the other vice versa. It is therefore necessary to supplement equations (71) and (72) with a condition determining exactly in which direction the energy is transferred. For the wave vector directed from the first to the second medium this condition is as follows

$$\frac{\partial H}{\partial \mathbf{k}}\,\mathbf{v} > 0\,. \tag{73}$$

To calculate the trajectory of a specific ray, its initial direction and point of emanation must be specified and the set of equations (68), (69) is integrated by eliminating the variable τ and taking into account the initial conditions. Then, the tensor n obtained by the coordinate transformation and the unit tensor are substituted into expression (70) to give, respectively, the trajectories $\mathbf{k}(\mathbf{x})$ of the ray inside and outside of the shell, which should be matched using the conditions (71)–(73).

Considering as an example a ray in a spherical cloaking shell, the tensor n in Cartesian coordinates is given by

$$n = \frac{b}{b-a}\left(I - \frac{2ar - a^2}{r^4}\,\mathbf{r}\otimes\mathbf{r}\right), \tag{74}$$

where a (b) is the inner (outer) radius of the shell, and $\mathbf{r}\otimes\mathbf{r}$ is the outer self-product of the radius vector $\mathbf{r}$ [71]. The outer product of vectors $\mathbf{x}$ and $\mathbf{y}$ is defined as the multiplication of a column vector by a row vector, namely

$$\mathbf{x}\otimes\mathbf{y} = \begin{pmatrix} x_1 \\ x_2 \\ x_3 \end{pmatrix}(y_1\,y_2\,y_3) = \begin{pmatrix} x_1y_1 & x_1y_2 & x_1y_3 \\ x_2y_1 & x_2y_2 & x_2y_3 \\ x_3y_1 & x_3y_2 & x_3y_3 \end{pmatrix}. \tag{75}$$

Substituting Eqn (74) into Eqn (70) and for simplicity choosing $f(\mathbf{x}) = (b-a)/2b$ as an arbitrary function in formula (70), the Hamiltonian for the spherical shell is found to be

$$H = \frac{1}{2}\,\mathbf{k}\mathbf{k} - \frac{1}{2}\,\frac{2ar - a^2}{r^4}(\mathbf{x}\mathbf{k})^2 - \frac{1}{2}\left[\frac{b(r-a)}{r(b-a)}\right]^2, \tag{76}$$

where r is the absolute value of the vector $\mathbf{x}$.

Taking derivatives yields

$$\frac{\partial H}{\partial \mathbf{k}} = \mathbf{k} - \frac{2ar - a^2}{r^4}(\mathbf{x}\mathbf{k})\mathbf{x}\,, \tag{77}$$

$$\frac{\partial H}{\partial \mathbf{x}} = -\frac{2ar - a^2}{r^4}(\mathbf{x}\mathbf{k})\mathbf{k} + \frac{3ar - 2a^2}{r^6}(\mathbf{x}\mathbf{k})^2\mathbf{x} - \left(\frac{b}{b-a}\right)^2\left(\frac{ar - a^2}{r^4}\right)\mathbf{x}\,. \tag{78}$$

Dividing Eqn (78) by Eqn (77) and integrating the resulting expression using the initial conditions, we find the trajectory of the ray in the cloaking shell. The numerical integration for a number of rays with different exit points yields the trajectories depicted in Fig. 1.

III. Historical remarks: is wave flow cloaking a decades-old idea?

As we have shown, wave flow cloaking is based on a quite transparent physical idea and relies on fairly simple mathematics and so — as far as its simplest version, a cloaking shell with $0 < \varepsilon < 1$ and $\mu = 1$, is concerned — could have been suggested and tested long before the work of J Pendry and coworkers [1, 2]. If anything, there was sufficient knowledge for this: for example, the trajectories of rays in an arbitrary, spherically symmetric, radially inhomogeneous medium had been quite thoroughly investigated as far back as the mid-20th century for a number of applications, including the spherical Luneburg–Maxwell fisheye lens [72, 73], the explanation of mirages (see above) [74], and long-range radio communication [75]. A long-known phenomenon in long-range radio communication, and one very close to cloaking, is so-called critical refraction. The essence of this effect is that the curvature of the surface a ray bends around is compensated for by variation in the refractive index, with the result that the rays become straight — which is exactly what makes a surface protrusion invisible.

There is indeed literature evidence that, supposedly, experiments on achieving invisibility for a large-sized object were performed in the US using the wave flow method and in connection with which the name of Albert Einstein himself is mentioned.

Specifically, or according to the claims made in near-scientific belles lettres, the USS Eldridge DE (Destroyer Escort) 173 was experimented on in 1943 with the goal of making it invisible for radar — the so-called Philadelphia Experiment (aka Project Rainbow) which, all claims notwithstanding and with no official confirmation from the U.S. Navy, is still considered a hoax.

The mysterious event has been the subject of two dozen or so books, and in 1984, The *Philadelphia Experiment*, a hit movie by Stewart Raffill, appeared on screens all over the world. Some information on the Philadelphia Experiment can also be found in the popular online encyclopedia *Wikipedia* at http://en.wikipedia.org/wiki/Philadelphia_Experiment where, incidentally, metamaterial-based cloaking is mentioned. (A reader with knowledge of Russian may also turn to Refs [76, 77].)

Briefly, at the heart of the experiment were several high-frequency transformers which were to be installed and simultaneously turned on aboard the destroyer — with the idea that the powerful high-frequency fields would produce high enough ionization of the air around the ship (plasma being exactly a medium where $0 < \varepsilon < 1$ and $\mu = 1$). To quote from Ref. [77], the idea was "to generate great electromagnetic field domains which, when properly configured, would be able to bend light and radio waves around the ship", thus making it invisible to enemy observers. Further on, "the bending of light by 10 percent" is mentioned. And still

USS *Eldridge* Destroyer Escort 173.

Albert Einstein in the company of navy officers, 24 July 1943. (Taken from Ref. [78].)

further, the effects discussed "included the ionization of the surrounding air, a 'boiling' of the water, and a 'Zeemanizing' of the atoms." Similar information can be gleaned from book [78].

Intriguingly, though, unintended and unplanned effects occurred during the experiment: in the optical range, the ship vanished into fog and became virtually invisible; at the very moment of disappearance, it was allegedly seen elsewhere, in the town of Norfolk, and, upon returning, terrible things happened to the crew: many of them suffered severe burns or died.

It is argued that Albert Einstein, Robert Oppenheimer, John von Neumann, and Nikola Tesla were invited to work out and direct these experiments. For example, Albert Einstein was often seen in the company of navy men in those years.

Explanations of what really happened to the destroyer abound, but are mostly too absurd even to be mentioned in a respected physics journal. According to some, suffice it to say, Einstein and Oppenheimer were invited as experts in practical antigravitation (!!) and quantum teleportation and their task was first to 'decompose' the ship into individual atoms, then, by using antigravitation, transfer the atoms to somewhere else, and there to puzzle them back together. As for Tesla, his role was to establish communications with extraterrestrial civilizations.

Whether or not this legend is based on real-life experiments will not be discussed here. What is important to us is that information about such experiments first leaked into print in 1964, implying that it was long before J Pendry, already in 1964 or at least in 1979 (according to Ref. [78]), that journalists learned from somebody that a large-scale object could be rendered invisible by making rays bend around it. Journalists understood this!

It is perhaps worth explaining what the mysterious word 'Zeemanizing' we mentioned a few paragraphs back means. [Interestingly, the Russian authors of Refs [76, 77] failed to translate it into Russian, and, it seems, the authors of Ref. [78] did not understand it, as the quotation marks around the word indicate. Suffice it to say that the word 'zeeman' in some West-European (e.g., Dutch) languages means 'sailor'.] This term, as any educated physicist will easily realize, refers to the magnetic Zeeman splitting of the electron and nuclear levels in the atoms constituting the medium, an effect which clearly affects the refractive properties of the medium at the energy-sublevel transition frequency. But this frequency, as calculated for magnetic fields used in warship demagnetization devices that were employed during WWII as an antimine measure, lies exactly in the radar frequency range, so it is now clear where the need for 'boiling water' came from. The point is that Zeeman splitting occurs only in atoms and molecules with unpaired electrons, but N_2, O_2, H_2, and He, the major components of air, have all their valence electrons paired, which makes Zeeman splitting forbidden. The 'Zeemanization' of the air requires that either it be ionized or dissociated or that some of its components be excited, both of which require huge energy depositions. One simple solution might be to have the ambient air around the ship saturated with sea water vapor with its asymmetric metal-chloride molecules.

Exactly which method — air ionization near the plasma frequency cutoff or the magnetic 'Zeemanization' of sea water vapor and spray — was primarily used to bend radar rays to achieve invisibility for radars, we do not know. But the term 'Zeemanization' enables a fairly accurate dating of when the idea of how to make a ship-sized object invisible first arose. The reader may have already guessed that there is a special term for this, the electron paramagnetic (or spin) resonance (EPR or ESR), an effect which was discovered by E K Zavoisky in 1944 [79], exactly in salt (metal-chloride) solutions; in the 1950s, EPR was already a ubiquitous term. Hence, the term 'Zeemanization' could only be used by a professional well-versed in the essence of EPR, while still lacking proper wording — which means the 1940s. Incidentally, E K Zavoisky himself pointed out more than once (see Ref. [80]) that some foreign researchers had conceived the idea of the effect before him and indeed had attempted to detect it but failed.

To summarize, it can be said that the favored choice must have been air ionization because, in addition to other practical difficulties in dealing with the Zeeman effect, the refractive index changes little near the resonance.

This being so, the role of the project leader scientists becomes clear. Einstein and Oppenheimer were needed exactly because of their authoritative expertise in space metrics and coordinate transformations. Von Neumann could have been instrumental in organizing plasma profile computations and the calculation of energy expenditure needed to implement the coordinate transformation. The most likely task for Tesla was the installation and tuning of HF inductors (known among experimentalists as Tesla transformers [81]) for the ionization of the ambient air.

Thus, it can be argued that at least a few decades ago the concept of wave flow cloaking was known to and understood by some specialists.

References

1. Pendry J B , Schurig D, Smith D R *Science* **312** 1780 (2006)
2. Schurig D et al. *Science* **314** 977 (2006)
3. Leonhardt U *New J. Phys.* **8** 118 (2006)
4. Leonhardt U, Philbin T G *New J. Phys.* **8** 247 (2006)
5. Rozanov N N *Priroda* (6) 3 (2008)
6. Litchinister N M et al. *Prog. Opt.* **51** 1 (2008)
7. Gulyaev Yu V, Lagar'kov A N, Nikitov S A *Vestn. Ross. Akad. Nauk* **78** 438 (2008) [*Herald Russ. Acad. Sci.* **78** 264 (2008)]
8. Dubinov A E, Mytareva L A *Elementy Fiziki 'Plashcha-nevidimki'* (Elements of the Physics of the 'Invisibility Cloak') (Sarov: SarFTI, 2009)

9. Veselago V G *Usp. Fiz. Nauk* **92** 517 (1967) [*Sov. Phys. Usp.* **10** 509 (1968)]
10. Veselago V G *Usp. Fiz. Nauk* **173** 790 (2003) [*Phys. Usp.* **46** 764 (2003)]
11. Bliokh K Yu, Bliokh Yu P *Usp. Fiz. Nauk* **174** 439 (2004) [*Phys. Usp.* **47** 393 (2004)]
12. Eleftheriades G V *Radio Sci. Bull.* (312) 57 (2005)
13. Veselago V et al. *J. Comp. Theor. Nanosci.* **3** 189 (2006)
14. Soukoulis C M et al. *J. Phys. Condens. Matter* **20** 304217 (2008)
15. Maier S A *Plasmonics*: *Fundamentals and Applications* (New York: Springer, 2007)
16. Krowne C M, Zhang Y *Physics of Negative Refraction and Negative Index Materials* (Berlin: Springer, 2007)
17. Zouhdi S, Sihvola A, Vinogradov A P (Eds) *Metamaterials and Plasmonics*: *Fundamentals, Modelling, Applications* (Dordrecht: Springer, 2009)
18. Silin R A *Neobychnye Zakony Prelomleniya i Otrazheniya* (Unusual Laws of Refraction and Reflection) (Moscow: Fazis, 1999)
19. Belotelov V I, Zvezdin A K *Fotonnye Kristally i Drugie Metamaterialy* (Photonic Crystals and Other Metamaterials) Prilozhenie k zhurnalu Kvant (Kvant journal Supplement) (Moscow: Byuro Kvantum, 2006)
20. Schurig D, Pendry J B, Smith D R *Opt. Express* **14** 9794 (2006)
21. Cummer S A et al. *Phys. Rev. E* **74** 036621 (2006)
22. Yan W, Yan M, Qiu M *Appl. Phys. Lett.* **93** 021909 (2008)
23. Cai W et al. *Appl. Phys. Lett.* **91** 111105 (2007)
24. Ma H et al. *Phys. Rev. A* **77** 013825 (2008)
25. Kwon D-H, Werner D H *Appl. Phys. Lett.* **92** 013505 (2008)
26. Kwon D-H, Werner D H *Appl. Phys. Lett.* **92** 113502 (2008)
27. Jiang W X et al. *J. Phys. D* **41** 085504 (2008)
28. Rahm M et al. *Photon. Nanostruct. Fund. Appl.* **6** 87 (2008)
29. Ma H et al. *Phys. Rev. E* **78** 036608 (2008)
30. Jiang W X et al. *Phys. Rev. E* **77** 066607 (2008)
31. Yao K, Li C, Li R *Appl. Phys. B* **96** 355 (2009)
32. Luo Y et al. *J. Phys. D* **41** 235101 (2008)
33. Luo Y et al. *Phys. Rev. B* **78** 125108 (2008)
34. Jiang W X et al. *Appl. Phys. Lett.* **93** 194102 (2008)
35. Li J, Pendry J B *Phys. Rev. Lett.* **101** 203901 (2008)
36. Liu R et al. *Science* **323** 366 (2009)
37. Hua M et al. *Chinese Phys. B* **18** 1025 (2009)
38. Zhang J et al. *Phys. Rev. B* **77** 035116 (2008)
39. Ma H et al. *Appl. Phys. Lett.* **94** 103501 (2009)
40. Luo Y et al. *Phys. Rev. B* **77** 125127 (2008)
41. Chen H et al. *Phys. Rev. Lett.* **99** 063903 (2007)
42. Ruan Z et al. *Phys. Rev. Lett.* **99** 113903 (2007)
43. Meng F-Y et al. *Appl. Phys. A* **95** 881 (2009)
44. Wu Q et al. *Appl. Phys. A* **95** 335 (2009)
45. Milton G W, Briane M, Willis J R *New J. Phys.* **8** 248 (2006)
46. Chen H, Chan C T *Appl. Phys. Lett.* **91** 183518 (2007)
47. Yang Z et al. *Phys. Rev. Lett.* **101** 204301 (2008)
48. Cheng Y, Liu X J *Appl. Phys. A* **94** 25 (2009)
49. Zhang S et al. *Phys. Rev. Lett.* **100** 123002 (2008)
50. Greenleaf A et al. *Phys. Rev. Lett.* **101** 220404 (2008)
51. Katsenelenbaum B Z *Radiotekh. Elektron.* **53** 673 (2008) [*J. Commun. Technol. Electron.* **53** 639 (2008)]
52. Katsenelenbaum B Z *Radiotekh. Elektron.* **54** 308 (2009) [*J. Commun. Technol. Electron.* **54** 292 (2009)]
53. Katsenelenbaum B Z, Voitovich N N *IEEE Trans. Antennas Propag.* **57** 2123 (2009)
54. Alù A, Engheta N *Phys. Rev. E* **78** 045602(R) (2008)
55. Silveirinha M G, Alù A, Engheta N *Phys. Rev. B* **78** 205109 (2008)
56. Alù A, Engheta N *Phys. Rev. Lett.* **102** 233901 (2009)
57. Smolyaninov I I, Hung Y J, Davis C C *Opt. Lett.* **33** 1342 (2008)
58. Pendry J B *Phys. Rev. Lett.* **85** 3966 (2000)
59. Pendry J B, Ramakrishna S A *J. Phys. Condens. Matter* **14** 8463 (2002)
60. Ramakrishna S A, Pendry J B *Phys. Rev. B* **69** 115115 (2004)
61. Luo Y et al. *Appl. Phys. Lett.* **95** 193506 (2009)
62. Lu W et al. *J. Phys. D* **42** 212002 (2009)
63. Nicolet A, Zolla F *Science* **323** 46 (2009)
64. Narimanov E E, Kildishev A V *Appl. Phys. Lett.* **95** 041106 (2009)
65. Greenleaf A et al. *Phys. Rev. Lett.* **99** 183901 (2007)
66. Frolov V P, Novikov I D *Phys. Rev. D* **42** 1057 (1990)
67. Visser M *Lorentzian Wormholes*: *from Einstein to Hawking* (Woodbury, NY: Am. Inst. of Phys., 1996)
68. Tretyakov S et al. *Phys. Rev. Lett.* **103** 103905 (2009)
69. Klimov K N et al. *Elektrodinamicheskii Analiz Dvumernykh Neodnorodnykh Sred i Plazmy* (Electrodynamic Analysis of Two-Dimensional Inhomogeneous Media and Plasma) (Moscow: MAKS Press, 2005)
70. Liu X et al. *Appl. Phys. Lett.* **95** 191107 (2009)
71. Schurig D, Pendry J B Smith D R *Opt. Express* **14** 9794 (2006)
72. Morgan S P *J. Appl. Phys.* **29** 1358 (1958)
73. Cornbleet S *Microwave Optics*: *The Optics of Microwave Antenna Design* (London: Academic Press, 1976) [Translated into Russian (Moscow: Svyaz, 1980)]
74. Fraser A B, Mach W H *Sci. Am.* **234** (1) 102 (1976); *Usp. Fiz. Nauk* **124** 333 (1978)
75. Feinberg E L *Rasprostranenie Radiovoln Vdol' Zemnoi Poverkhnosti* (Radio Wave Propagation Along the Earth's Surface) (Moscow: Fizmatlit, 1999)
76. Kuzovkin A S, Nepomnyashchii N N *Chto Sluchilos' s Esmintsem 'Eldridzh'* (What Happened to Torpedo-Boat 'Eldridge') (Znak Voprosa Series, Issue 3) (Moscow: Znanie, 1991)
77. Telitsyn V *Nikola Tesla i Taina Filadel'fiiskogo Eksperimenta* (Nikola Tesla and the Mystery of the Philadelphia Experiment) (Moscow: Yauza–Eksmo, 2009)
78. Moore W, Berlitz Ch *The Philadelphia Experiment*: *Project Invisibility* (London: Souvenir Press Ltd., 1979)
79. Zavoisky E *J. Phys. USSR* **8** 377 (1944)
80. Al'tshuler S A, Zavoiskii E K, Kozyrev B M *Izv. Akad. Nauk SSSR Ser. Fiz.* **20** 1199 (1956)
81. El'chaninov A S et al. *Relyativistskaya Vysokochastotnaya Elektronika*: *Problema Povysheniya Moshchnosti i Chastoty Izlucheniya* (Relativistic High-Frequency Electronics: The Problem of Increasing the Power and Frequency of Radiation) (Gor'kii: IPF AN SSSR, 1981)